

Learning High-Dimensional McKean-Vlasov Forward-Backward Stochastic Differential Equations with General Distribution Dependence

Jiequn Han*

Ruimeng Hu[†]Jihao Long[‡]

September 20, 2023

Abstract

One of the core problems in mean-field control and mean-field games is to solve the corresponding McKean-Vlasov forward-backward stochastic differential equations (MV-FBSDEs). Most existing methods are tailored to special cases in which the mean-field interaction only depends on expectation or other moments and thus is inadequate to solve problems when the mean-field interaction has full distribution dependence.

In this paper, we propose a novel deep learning method for computing MV-FBSDEs with a general form of mean-field interactions. Specifically, built on fictitious play, we recast the problem into repeatedly solving standard FBSDEs with explicit coefficient functions. These coefficient functions are used to approximate the MV-FBSDEs' model coefficients with full distribution dependence, and are updated by solving another supervising learning problem using training data simulated from the last iteration's FBSDE solutions. We use deep neural networks to solve standard BSDEs and approximate coefficient functions in order to solve high-dimensional MV-FBSDEs. Under proper assumptions on the learned functions, we prove that the convergence of the proposed method is free of the curse of dimensionality (CoD) by using a class of integral probability metrics (IPMs) previously developed in [Han, Hu and Long, arXiv:2104.12036]. The proved theorem shows the advantage of the method in high dimensions. We present the numerical performance in high-dimensional MV-FBSDE problems, including a mean-field game example of the well-known Cucker-Smale model whose cost depends on the full distribution of the forward process.

Keywords: McKean-Vlasov FBSDE, fictitious play, mean-field games, Deep BSDE, maximum mean discrepancy, convergence analysis.

1 Introduction

The McKean-Vlasov forward-backward stochastic differential equations (MV-FBSDEs) arise as natural formulations for mean-field games (MFGs) and mean-field control (MFC) problems. Initially introduced by Lasry-Lions [33, 34, 35] and Huang-Malhame-Caines [30, 31], MFG studies the strategic decision-making by a continuum of homogeneous agents where each of them aims to maximize her/his own goal. Since each agent is infinitesimal, the law of states processes is considered fixed

*Center for Computational Mathematics, Flatiron Institute, New York, NY 10010, jiequnhan@gmail.com.

[†]Department of Mathematics, and Department of Statistics and Applied Probability, University of California, Santa Barbara, CA 93106-3080, rhu@ucsb.edu.

[‡]The Program in Applied and Computational Mathematics, Princeton University, Princeton, NJ 08544-1000, jihao@princeton.edu.

while an agent optimizes her cost functional. Therefore, it is merely a standard optimal control problem plus a fixed point argument (that the distribution of the solution is equal to the distribution one starts from). From a slightly different perspective, MFC analyzes the optimal control of stochastic differential equations (SDEs) of the McKean-Vlasov type, which can be interpreted as the limiting regime of a cooperative game among large population agents. This objective adds an extra optimization layer to the fixed point, that is, the law of state processes changes as one optimizes her goal. Despite their differences, both problems can be solved via analyzing the MV-FBSDEs using the Pontryagin maximum principle [9, 11], and both solutions serve as approximate equilibrium strategies for large populations of individuals whose interactions and objective functions are of the mean-field type. To further explain their differences and relations, we refer readers to [11, Section 6].

In this paper, we are interested in developing efficient deep learning methods and analyzing the numerical convergence for the following MV-FBSDEs,

$$\begin{cases} dX_t = b(t, X_t, Y_t, Z_t, \mathcal{L}(X_t, Y_t, Z_t)) dt + \sigma(t, X_t, Y_t, Z_t, \mathcal{L}(X_t, Y_t, Z_t)) dW_t, & X_0 = x_0, \\ dY_t = -h(t, X_t, Y_t, Z_t, \mathcal{L}(X_t, Y_t, Z_t)) dt + Z_t dW_t, & Y_T = g(X_T, \mathcal{L}(X_T)), \end{cases} \quad (1)$$

on a finite horizon $[0, T]$, where $\mathcal{L}(\cdot)$ denotes the marginal law of a process, and (b, σ, h, g) are measurable functions of compatible dimensions, with specific forms detailed in Section 2. Particularly, we shall focus on computing MV-FBSDEs in high dimensions with a general form of mean-field interactions, while most existing methods only deal with special cases when the mean-field interaction is described via expectations or other moments.

Theoretically, existence and uniqueness results for MV-FBSDEs have been recently developed [8, 9, 10], mostly tackled by a compactness argument and fixed point theorems. In particular, when σ is free of Z_t and $\mathcal{L}(Z_t)$, under suitable conditions [11, Theorem 4.29, Remark 4.30], the MV-FBSDEs (1) admit a solution with a decoupling field

$$Y_t = u(t, X_t), \quad Z_t = v(t, X_t) \quad (2)$$

where $v(t, x) = \partial_x u(t, x) \sigma(t, x, u(t, x), (I_d, u(t, \cdot))(\mathcal{L}(X_t)))$. Several numerical algorithms have been designed for solving MV-FBSDEs, including a recursive local Picard iteration method [13], cubature based algorithm for the decoupled setting [15], and deep learning methods [12, 21]. Most of the work, with or without analysis, only present numerical examples of a special type of mean-field interaction, that is, (b, σ, h, g) depends on \mathcal{L} only through its expectation. On a related topic, MFGs and MFC problems have also been solved using partial differential equations and using neural networks for high-dimensional problems; for instance, see [2, 45, 44, 1].

The work most closely related to ours is [21]. It solves the MV-FBSDEs using deep learning, and the dependence of the (b, σ, h, g) with respect to $\mathcal{L}(X_t, Y_t, Z_t)$ are solely in terms of expectations of the form $(\mathbb{E}[\varphi_1(X_t)], \mathbb{E}[\varphi_2(Y_t)], \mathbb{E}[\varphi_3(Z_t)])$ with some continuous functions φ_i . To do so, one is essentially estimating some equilibrium numbers $\int_y \varphi_i(y) \mu(dy)$ where μ is the law of the MV-FBSDE solution. Beyond mere dependency on moments, which is the scope of this paper, the goal is to learn equilibrium functions that depend on the distribution in a nonlinear way, e.g., functions in (t, x) of the form $\int_y \varphi(t, x, y) \mu(dy)$. This presents greater challenges in terms of both algorithm design and the method employed for representing these quantities.

Here we propose a novel deep learning method to solve high-dimensional MV-FBSDEs, leveraging the idea of fictitious play [6, 7] and the existing machine learning BSDE solvers [16, 26, 27, 32], with the capability of dealing with general mean-field dependence (not only moments). The main contributions are:

1. Motivated by the fixed-point nature of MV-FBSDEs, we use fictitious play and solve

$$\begin{cases} dX_t^k = b(t, \Theta_t^k, \mathcal{L}(\Theta_t^{k-1})) dt + \sigma(t, \Theta_t^k, \mathcal{L}(\Theta_t^{k-1})) dW_t, & X_0 = x_0, \\ dY_t^k = -h(t, \Theta_t^k, \mathcal{L}(\Theta_t^{k-1})) dt + Z_t^k dW_t, & Y_T = g(X_T^k, \mathcal{L}(X_T^{k-1})), \end{cases} \quad (3)$$

among solutions in the form of decoupling fields (that is, search for some deterministic functions u^k, v^k which are viewed as approximations to u, v defined in (2) such that $Y_t^k = u^k(t, X_t^k), Z_t^k = v^k(t, X_t^k)$), iteratively via existing BSDE solvers, where $\Theta^k = (X^k, Y^k, Z^k)$ is the short notation of the solution to (3), and is understood as the k^{th} iteration approximation of (X, Y, Z) in (1). To speed up the simulation of (X^k, Y^k) for the BSDE solver, we propose to use neural networks to learn the maps $(t, X_t, Y_t, Z_t) \mapsto (b, \sigma, h, g)$ by supervised learning when they depend fully on any distribution. Numerically, the function values (also known as the “labels”) are approximated via replacing $\mathcal{L}(\cdot)$ by the corresponding empirical distribution of the solution from the last iteration and the learned maps are updated after each iteration.

2. We prove the convergence for the proposed algorithm. Using the integral probability metrics proposed in [25], the difference between the learned process and the solution can be sufficiently small and free of the curse of dimensionality, subject to sufficient smoothness of the learned functions, sufficient iterations of fictitious play, and sufficiently small time steps.
3. We introduce a mean-field game of the Cucker-Smale model where the cost depends on the full distribution of the forward process. We provide numerical benchmarks and hope this will facilitate the further study of numerical algorithms for MV-FBSDEs.

The rest of the paper is organized as follows. In Section 2, we review the idea of fictitious play and two existing deep learning (DL)-based BSDE solvers: Deep BSDE and DBDP, and describe our proposed algorithm. Section 3 provides the convergence analysis for the proposed algorithm. Two numerical examples are presented in Section 4. The first one is ten-dimensional with an analytic solution to benchmark. It is worth mentioning that the first example is not the frequently used MV-FBSDEs associated with linear quadratic problems that have been extensively benchmarked in the literature. In the second example, we study a mean-field flocking problem under the Cucker-Smale model. The mean-field interaction there involves the whole distribution of the state processes. We conclude in Section 5.

Notations. Throughout the paper, we fix a probability space $(\Omega, \mathcal{F}, \mathbb{P})$ that supports q -dimensional Brownian motions $(W_t^{n,k})_{t \in [0, T]}$, $n = 1, \dots, N$, $k = 1, \dots$ and $(W_t)_{t \in [0, T]}$ on the fixed horizon $[0, T]$. Let $\mathbb{F} := (\mathcal{F}_t)_{t \in [0, T]}$ be the natural filtration associated with W . We denote by $\mathbb{H}^2(\mathbb{R}^d)$ the space

$$\mathbb{H}^2(\mathbb{R}^d) = \left\{ x \text{ is } \mathbb{R}^d\text{-valued progressively measurable: } \mathbb{E} \int_0^T \|x_t\|^2 ds < \infty \right\},$$

where $\|\cdot\|$ denote the ℓ^2 norm. The space $\mathbb{S}^2(\mathbb{R}^d)$ denotes all the continuous \mathbb{R}^d -valued progressively measurable processes x_t such that $\mathbb{E}[\sup_{0 \leq t \leq T} \|x_t\|^2] < \infty$. We fix the dimension of (X_t, Y_t, Z_t) in (1) by $X_t \in \mathbb{R}^d$, $Y_t \in \mathbb{R}^p$ and $Z_t \in \mathbb{R}^{p \times q}$, and denote by ν_t and μ_t the empirical measures of (X_t, Y_t, Z_t) and X_t , respectively.

Denote by $\mathcal{P}(\mathbb{R}^d)$ the space of probability measures on \mathbb{R}^d , and by $\mathcal{P}^s(\mathbb{R}^d)$ a subspace of $\mathcal{P}(\mathbb{R}^d)$ with finite s^{th} -moments, *i.e.*, $\mu \in \mathcal{P}^s(\mathbb{R}^d)$ if and only if

$$M_s(\mu) := \left(\int_{\mathbb{R}^d} \|x\|^s d\mu(x) \right)^{1/s} < +\infty.$$

We will mostly work with probability measures with finite second moments, *i.e.*, $\mathcal{P}^2(\mathbb{R}^d)$.

2 Deep Learning Algorithm for McKean-Vlasov FBSDEs

Compared to the standard FBSDEs problem, solving the MV-FBSDEs (1) faces two additional difficulties:

1. The law $\mathcal{L}(X_t, Y_t, Z_t)$ is unknown a priori, but determined as a fixed-point;
2. Even given the law $\mathcal{L}(X_t, Y_t, Z_t)$, the dependence of coefficient functions (b, σ, h, g) on $\mathcal{L}(X_t, Y_t, Z_t)$ can be so complicated that the resulting FBSDEs are computationally challenging to solve.

To overcome the first difficulty, we use the idea of fictitious play. Fictitious play is originally introduced by Brown [6, 7] as a learning process for finding Nash equilibrium in static games, and has attracted many attentions and has been used in machine learning algorithms and theory for various settings; see, for instance, in [29, 23, 24, 18, 47, 48, 37, 28]. Such problems usually require finding an “equilibrium” quantity Q^* . In turn, one could start with an initial guess $Q^{(0)}$ of this “equilibrium”, use it to solve the problem, and update the guess $Q^{(1)}$ accordingly. Then the problem with a given $Q^{(k)}$ is solved repeatedly, producing a sequence $Q^{(0)}, Q^{(1)}, \dots, Q^{(k)}, \dots$ which one hopes to have a limit Q^* . In N -player games, the quantity is the Nash equilibrium strategy, while in mean-field games, it is the law of the optimal state processes. In this paper, it will be the flow of measures of (X_t, Y_t, Z_t) . Note that the idea of fictitious play is very much in line with the theoretical construction of the solution to (1), which is usually done by recasting it into a well-posed fixed point problem over the argument $\mathcal{L}(X_t, Y_t, Z_t)$. There, the first step is to use some fixed distribution as an input and then solve it as a standard FBSDE, and the goal is to find a fixed point for the map from the input distribution to the law of the standard FBSDE in appropriate spaces of functions and measures. To overcome the second difficulty, we observe that $\mathcal{L}(X_t, Y_t, Z_t)$ are deterministic functions of time t , so we can view m_1 and m_2 in (15) as functions of (t, x) , and similarly view m_3 as a function of x . Therefore, we use supervised learning to learn these maps directly, given the latest empirical estimate of $\mathcal{L}(X_t, Y_t, Z_t)$.

Now we are ready to present the proposed algorithm. To ease the notation, we define the processes $\Theta \triangleq (X, Y, Z)$ where (X, Y, Z) are in (1), and define $\mathbb{R}^\theta \triangleq \mathbb{R}^d \times \mathbb{R}^p \times \mathbb{R}^{p \times q}$ which the space Θ_t lies in. In the sequel, any sub/superscript added to Θ are automatically applied to (X, Y, Z) , *e.g.*, $\Theta_{t_i}^k = (X_{t_i}^k, Y_{t_i}^k, Z_{t_i}^k)$ represents the time t_i value of the MV-FBSDEs solved at the k^{th} iteration of fictitious play.

2.1 The Deep MV-FBSDE Algorithm

We first assume the following structures for functions (b, σ, h, g) . Let $m_1, m_2 : [0, T] \times \mathbb{R}^d \times \mathcal{P}^2(\mathbb{R}^\theta) \rightarrow \mathbb{R}^l$ and $m_3 : \mathbb{R}^d \times \mathcal{P}^2(\mathbb{R}^d) \rightarrow \mathbb{R}^l$ be vector-valued functions such that

$$\begin{aligned} b &= b(t, \Theta_t, m_1(t, X_t, \mathcal{L}(\Theta_t))), & \sigma &= \sigma(t, X_t), \\ h &= h(t, \Theta_t, m_2(t, X_t, \mathcal{L}(\Theta_t))), & g &= g(X_T, m_3(X_T, \mathcal{L}(X_T))). \end{aligned} \tag{4}$$

As introduced above, our algorithm is iterative over the solution (X_t, Y_t, Z_t) and their empirical measures. We use superscripts $k = 1, 2, \dots$ to index such iterations. In each iteration stage, the algorithm performs the following three steps.

Step 1. Update the approximation to distributions $\mathcal{L}(\Theta)$ ¹ Given the latest approximation to the solution $Y_0 \approx u^{k-1}(0, X_0), Z_t \approx v^{k-1}(t, X_t)$ and approximation to the distribution dependence $\widehat{m}_1^{k-1}, \widehat{m}_2^{k-1}, \widehat{m}_3^{k-1}$ (see the second step for how these functions are constructed; when $k = 1$,

¹The iteration can also proceed with a different order of three steps, as long as some proper initial conditions corresponding to $k = 0$ are provided.

these functions are defined by the neural networks (NNs) with randomly initialized weights), we consider the following forward SDEs for $(\tilde{X}_t^{k-1}, \tilde{Y}_t^{k-1})$ (the superscript $k-1$ denotes the $(k-1)^{th}$ stage):

$$\begin{cases} d\tilde{X}_t^{k-1} = b(t, \tilde{\Theta}_t^{k-1}, \hat{m}_1^{k-1}(t, \tilde{X}_t^{k-1})) dt + \sigma(t, \tilde{X}_t^{k-1}) dW_t, & \tilde{X}_0^{k-1} = \xi, \\ d\tilde{Y}_t^{k-1} = -h(t, \tilde{\Theta}_t^{k-1}, \hat{m}_2^{k-1}(t, \tilde{X}_t^{k-1})) dt + v^{k-1}(t, \tilde{X}_t^{k-1}) dW_t, & \tilde{Y}_0^{k-1} = u^{k-1}(0, \tilde{X}_0^{k-1}). \end{cases} \quad (5)$$

and use the corresponding distribution

$$\nu_t^{k-1} = \mathcal{L}(\tilde{\Theta}_t^{k-1}), \quad \mu_T^{k-1} = \mathcal{L}(\tilde{X}_T^{k-1}),$$

for approximating $\mathcal{L}(\Theta_t)$ and $\mathcal{L}(X_T)$. In practice, we will further approximate ν_t^{k-1} and μ_T^{k-1} by their empirical versions, as detailed in Section 2.3.

Step 2. Approximate the distribution dependence m_1 , m_2 and m_3 Given the latest estimates of $\mathcal{L}(\Theta_t)$ and $\mathcal{L}(X_T)$, we can view m_1, m_2 as functions of (t, x) and m_3 as a function of x . Naturally, we can parameterize these functions using neural networks and optimize through supervised learning. After the $(k-1)^{th}$ stage, we optimize

$$\begin{aligned} & \inf_{\mathbf{m}_1} \int_0^T \mathbb{E} \|m_1(t, \tilde{X}_t^{k-1}, \nu_t^{k-1}) - \mathbf{m}_1(t, \tilde{X}_t^{k-1})\|^2 dt, \\ & \inf_{\mathbf{m}_2} \int_0^T \mathbb{E} \|m_2(t, \tilde{X}_t^{k-1}, \nu_t^{k-1}) - \mathbf{m}_2(t, \tilde{X}_t^{k-1})\|^2 dt, \\ & \inf_{\mathbf{m}_3} \mathbb{E} \|m_3(\tilde{X}_T^{k-1}, \mu_T^{k-1}) - \mathbf{m}_3(\tilde{X}_T^{k-1})\|^2, \end{aligned} \quad (6)$$

where \mathbf{m}_i , $i = 1, 2, 3$ are searched over a class of NNs (to be specified in Section 4). The optimized NNs, denoted by \hat{m}_1^k , \hat{m}_2^k and \hat{m}_3^k respectively, will be needed in Step 3 below, and Step 1 in the next stage.

Step 3. Solve the standard FBSDEs The FBSDEs to be solved at the k^{th} stage for (X_t^k, Y_t^k, Z_t^k) read as

$$\begin{cases} dX_t^k = b(t, \Theta_t^k, \hat{m}_1^k(t, X_t^k)) dt + \sigma(t, X_t^k) dW_t, & X_0^k = \xi, \\ dY_t^k = -h(t, \Theta_t^k, \hat{m}_2^k(t, X_t^k)) dt + Z_t^k dW_t, & Y_T^k = g(X_T^k, \hat{m}_3^k(X_T^k)), \end{cases} \quad (7)$$

and one aims to find the optimal NNs ψ^k and ϕ^k that parameterize Y_0^k and Z_t^k , respectively. The exact way of obtaining ψ^k and ϕ^k depends on the particular BSDE solver that one will use, and this will be presented in Section 2.2. The functions ψ^k and ϕ^k are considered as approximations to the decoupling field u^k and v^k of equation (3).

Remark 2.1. A novel step in our algorithm is Step 2 (the supervised learning on m_i). It produces m_i 's proxy \hat{m}_i , $i = 1, 2, 3$, thus provides quick evaluations of m_i . This is crucial in our ‘‘Step 3: Solve the Standard FBSDEs’’. If such \hat{m}_i is not available, one needs to solve the following system

$$\begin{cases} dX_t^k = b(t, \Theta_t^k, m_1(t, X_t^k, \mathcal{L}(\Theta_t^k))) dt + \sigma(t, X_t^k) dW_t, & X_0^k = \xi, \\ dY_t^k = -h(t, \Theta_t^k, m_2(t, X_t^k, \mathcal{L}(\Theta_t^k))) dt + Z_t^k dW_t, & Y_T^k = g(X_T^k, m_3(X_T^k, \mathcal{L}(X_T^k))), \end{cases}$$

in Step 3. However, by its definition (the dependence on $\mathcal{L}(\cdot)$), it can only be approximated via empirical distributions, thus very time-consuming compared to the quick evaluation of $\hat{m}_i(t, x)$.

Remark 2.2. Notice that when we learn $(\widehat{m}_1^k, \widehat{m}_2^k, \widehat{m}_3^k)$ in the optimization problem (6), the difference is evaluated along \widetilde{X}_t^{k-1} ; while when we solve the FBSDEs (7), we plug in X_t^k . The mismatch between the distribution of the random variables that we use to learn the functions and the random variables that we use to solve FBSDEs will lead to theoretical and numerical difficulty, and this is the very reason why we limit (b, σ, h, g) in the forms (4). Under this assumption, the distribution of X_t^k is absolutely continuous with respect to the distribution of \widetilde{X}_t^{k-1} through the Girsanov theorem; hence we can use the errors under \widetilde{X}_t^{k-1} to control the errors under X_t^k ; see Lemma 3.8 for a detailed statement.

An alternative approach is that one could use $(\widehat{m}_1^k, \widehat{m}_2^k, \widehat{m}_3^k)$ in the other two steps the same way as in the second step, *i.e.*, replace $(\Theta_t^{k-1}, X_t^{k-1})$ by $(\Theta_t^{k-2}, X_t^{k-2})$ in equation (5) and (Θ_t^k, X_t^k) by $(\Theta_t^{k-1}, X_t^{k-1})$ in equation (7) in model coefficients (b, σ, h, g) . In this case, we will use the same random variables to learn the functions and to solve the FBSDEs and hence can handle more general setting on (b, σ, h, g) :

$$(b, h, \sigma) = (b, h, \sigma)(t, \Theta_t, m_1(t, \Theta_t, \mathcal{L}(\Theta_t))), \quad g = g(X_T, m_2(X_T, \mathcal{L}(X_T))).$$

However, if one wants to simulate a path of X_t^k , one needs to first simulate paths of $X_t^0, X_t^1, \dots, X_t^{k-1}$ under the same realization of Brownian motions, which will not be computationally efficient.

In a nutshell, there is a trade-off between the two choices, and we decide to go with the current choice (4) for the analysis in Section 3, since it is more numerically favorable.

2.2 BSDE Solvers

We now describe the numerical algorithm for solving the FBSDEs (7) in the inner stage of fictitious play. For the clarity of notations, we use generic FBSDEs

$$\begin{cases} dX_t = B(t, X_t, Y_t, Z_t) dt + \Sigma(t, X_t, Y_t, Z_t) dW_t, & X_0 = x_0, \\ dY_t = -H(t, X_t, Y_t, Z_t) dt + Z_t dW_t, & Y_T = G(X_T), \end{cases} \quad (8)$$

to describe the algorithm. We shall mainly consider two types of BSDE solvers that leverage neural networks and thus are suitable for high-dimensional settings.

The first algorithm is the Deep BSDE method [16, 26, 27], the first method designed for solving high-dimensional BSDEs and parabolic PDEs with neural networks (NNs). The Deep BSDE method solves the variational problem which is equivalent to (8),

$$\begin{aligned} & \inf_{Y_0, (Z_t)_{t \in [0, T]}} \mathbb{E} \|G(X_T) - Y_T\|^2, \\ \text{s.t. } & X_t = x_0 + \int_0^t B(s, X_s, Y_s, Z_s) ds + \int_0^t \Sigma(s, X_s, Y_s, Z_s) dW_s, \\ & Y_t = Y_0 - \int_0^t H(s, X_s, Y_s, Z_s) ds + \int_0^t Z_s dW_s. \end{aligned}$$

To solve the above variational problem numerically, the method works on a discretized version and parameterizes Y and Z at each t_i as functions of X_{t_i} using NNs. To fix the notation, we consider a partition π on the interval $[0, T]$ of size N_T : $0 = t_0 < t_1 < \dots < t_i < \dots < t_{N_T} = T$ and define $\Delta t_i := t_{i+1} - t_i$. Then we only need to minimize the L^2 difference between the simulated Y_T and

its target value $G(X_T)$:

$$\begin{aligned}
& \inf_{\psi \in \mathcal{N}', \{\phi_i \in \mathcal{N}_i\}_{i=0}^{N_T-1}} \mathbb{E} \|G(X_T) - Y_T\|^2, \\
s.t. \quad & X_0 = x_0, \quad Y_0 = \psi(X_0), \quad Z_{t_i} = \phi_i(X_{t_i}, Y_{t_i}), \\
& X_{t_{i+1}} = X_{t_i} + B(t_i, X_{t_i}, Y_{t_i}, Z_{t_i})\Delta t_i + \Sigma(t_i, X_{t_i}, Y_{t_i}, Z_{t_i})\Delta W_{t_i}, \\
& Y_{t_{i+1}} = Y_{t_i} - H(t_i, X_{t_i}, Y_{t_i}, Z_{t_i})\Delta t_i + Z_{t_i}\Delta W_{t_i},
\end{aligned} \tag{9}$$

where $\Delta W_{t_i} = W_{t_{i+1}} - W_{t_i}$ is the Brownian increment from t_i and t_{i+1} , an ψ and ϕ_i are functions in the hypothesis spaces \mathcal{N}' and \mathcal{N}_i that are generated by neural networks (NNs). Note that the above choice without ϕ_i 's dependence on Y is consistent with our goal of searching for the decoupling field (cf. (2)). However, in the rigorous justification of Deep BSDE [27], Y is needed for ϕ_i in the proof of coupled FBSDEs, thus we include it here.

The second algorithm we consider is the deep backward dynamic programming (DBDP) method [32]. The original DBDP [32] can only deal with the decoupled FBSDE in (8), that is, B and Σ are free of (Y_t, Z_t) , so does the presentation below. Accordingly, so far we can only apply the DBDP to MV-FBSDE problems in which b and σ are free of (Y_t, Z_t) ². Same as the Deep BSDE method, the DBDP method parameterizes Y_{t_i} and Z_{t_i} at each t_i as functions of X_{t_i} and solves optimization problems to get the optimal parameters. Instead of solving the global minimization problem (9) over the whole time interval in the Deep BSDE method, the DBDP method solves Y_{t_i} and Z_{t_i} sequentially and backwardly for $i = t_{N_T} - 1, \dots, 0$. Given the learnt functions $\psi_{t_{i+1}}^*$ representing $Y_{t_{i+1}}$ (by definition Y_T is replaced by $g(X_t)$ at $i = t_{N_T}$), the i^{th} problem is to train the neural networks ψ_i, ϕ_i via:

$$\begin{aligned}
& \inf_{\psi_i \in \mathcal{N}'_i, \phi_i \in \mathcal{N}_i} \mathbb{E} \left\| Y_{t_{i+1}} - Y_{t_i} + H(t_i, X_{t_i}, Y_{t_i}, Z_{t_i})\Delta t_i - Z_{t_i}\Delta W_{t_i} \right\|^2 \\
s.t. \quad & Y_{t_i} = \psi_i(X_{t_i}), \quad Y_{t_{i+1}}^* = \psi_{t_{i+1}}^*(X_{t_{i+1}}), \quad Z_{t_i} = \phi_i(X_{t_i}), \\
& X_{t_{i+1}} = X_{t_i} + B(t_i, X_{t_i})\Delta t_i + \Sigma(t_i, X_{t_i})\Delta W_{t_i}.
\end{aligned} \tag{10}$$

In practice, the objective (9) or (10) in these two methods is approximated by its Monte-Carlo counterpart and the (near-) optimal NN parameters that represent ψ^* and ϕ_i^* (or ψ_i^* and ϕ_i^* in DBDP) are obtained by stochastic gradient decent algorithms which require simulating a batch of Brownian paths at each update. To related to notations in Section 2.1 Step 3, they provide ϕ^k and ψ^k .

We remark that in the setting of MV-FBSDEs, the functions (b, h, g) may depend on $\mathcal{L}(\Theta_t)$ in complicated forms, which may bring challenges to solve the optimization problems (9) or (10). That is the reason we propose to use neural networks to approximate the dependence on the laws through (6) to make the resulting FBSDE easier to solve. For further numerical details and theoretical foundations of these two methods, we refer the readers to [16, 26, 27, 32].

2.3 Implementation Details

We now detail the algorithm outlined in Section 2.1. How the standard FBSDEs in the third step are numerically solved has been discussed in Section 2.2. So we will mainly present the numerical details of the other two steps. Same to the notations used in Section 2.2, we consider a partition π on the interval $[0, T]$ of size N_T : $0 = t_0 < t_1 < \dots < t_i < \dots < t_{N_T} = T$ with $\Delta t_i := t_{i+1} - t_i$. To

²The dependence on $\mathcal{L}(Y_t, Z_t)$ is fine as it will be approximated by \widehat{m}_1^k that does not depend on $\mathcal{L}(Y_t, Z_t)$. This is exactly the setting of the example in Section 4.1

update the distribution in the first step, we generate N samples of initial condition $\xi^{n,k-1}$ and N samples of Brownian motions $W_t^{n,k-1}$, $n = 1, \dots, N$ to simulate the forward SDEs (5) in discrete time:

$$\begin{cases} \tilde{X}_{t_{i+1}}^{n,k-1} = \tilde{X}_{t_i}^{n,k-1} + b(t_i, \tilde{\Theta}_{t_i}^{n,k-1}, \hat{m}_1^{k-1}(t_i, \tilde{X}_{t_i}^{n,k-1}))\Delta t_i + \sigma(t_i, \tilde{X}_{t_i}^{n,k-1})\Delta W_{t_i}^{n,k-1}, \\ \tilde{Y}_{t_{i+1}}^{n,k-1} = \tilde{Y}_{t_i}^{n,k-1} - h(t_i, \tilde{\Theta}_{t_i}^{n,k-1}, \hat{m}_2^{k-1}(t_i, \tilde{X}_{t_i}^{n,k-1}))\Delta t_i + v^{k-1}(t_i, \tilde{X}_{t_i}^{n,k-1})\Delta W_{t_i}^{n,k-1}, \end{cases} \quad (11)$$

with initial conditions $\tilde{X}_0^{n,k-1} = \xi^{n,k-1}$, $\tilde{Y}_0^{n,k-1} = u^{k-1}(0, \tilde{X}_0^{n,k-1})$ and define the empirical measures

$$\nu_{t_i}^{k-1} = \frac{1}{N} \sum_{n=1}^N \delta_{\tilde{\Theta}_{t_i}^{n,k-1}}, \quad \mu_T^{k-1} = \frac{1}{N} \sum_{n=1}^N \delta_{\tilde{X}_T^{n,k-1}}, \quad (12)$$

for approximating $\mathcal{L}(\Theta_t)$ at discretized timestamps t_i and $\mathcal{L}(X_T)$.

Next, we will use data obtained from (11) to construct the supervised learning problem in the second step to approximate the distribution dependence. By Monte Carlo sampling, we can approximate the problems in (6) with

$$\begin{aligned} & \inf_{\mathbf{m}_1} \sum_{1 \leq n \leq N} \sum_{0 \leq i \leq N_T-1} \|m_1(t_i, \tilde{X}_{t_i}^{n,k-1}, \nu_{t_i}^{k-1}) - \mathbf{m}_1(t_i, \tilde{X}_{t_i}^{n,k-1})\|^2, \\ & \inf_{\mathbf{m}_2} \sum_{1 \leq n \leq N} \sum_{0 \leq i \leq N_T-1} \|m_2(t_i, \tilde{X}_{t_i}^{n,k-1}, \nu_{t_i}^{k-1}) - \mathbf{m}_2(t_i, \tilde{X}_{t_i}^{n,k-1})\|^2, \\ & \inf_{\mathbf{m}_3} \sum_{1 \leq n \leq N} \|m_3(\tilde{X}_T^{n,k-1}, \mu_T^{k-1}) - \mathbf{m}_3(\tilde{X}_T^{n,k-1})\|^2. \end{aligned} \quad (13)$$

Given $(\hat{m}_1^k, \hat{m}_2^k, \hat{m}_3^k)$ solved from (13), we can solve the FBSDEs (7) using the introduced BSDE solvers. Taking the Deep BSDE method as the example, the whole deep learning algorithm for solving the MV-FBSDEs can be summarized below.

Algorithm 1 The Deep MV-FBSDEs method

Require: Input: the time partition $0 = t_0 < t_1 < \dots < t_i < \dots < t_{N_T} = T$, the number of paths N for simulating the SDEs, the initialization of the decoupling field $u^0(0, X_0)$, $v^0(t, X_t)$ and the distribution dependence $(\hat{m}_1^0, \hat{m}_2^0, \hat{m}_3^0)$

- 1: **for** $k = 1, 2, \dots$ **do**
 - 2: Simulate the forward SDEs (11) to collect the data $\tilde{X}_{t_i}^{n,k-1}, \tilde{Y}_{t_i}^{n,k-1}, \tilde{Z}_{t_i}^{n,k-1}$, $n = 1, \dots, N, i = 0, \dots, N_T$
 - 3: Define the empirical measures according to (12)
 - 4: Train $(\hat{m}_1^k, \hat{m}_2^k, \hat{m}_3^k)$ to solve the optimization problem (13)
 - 5: Train ψ^k and ϕ^k to solve the variational problem (9) corresponding to the FBSDEs (7)
 - 6: **end for**
-

3 Convergence Analysis

This section is dedicated to the numerical analysis of the algorithms proposed in Section 2, in particular, the justification of learning \hat{m}_i^k , $i = 1, 2, 3$ from (13). The metric we use here for measuring the convergence of distributions in $\mathcal{P}^2(\mathbb{R}^\theta)$ falls into the category of integral probability metrics [38], under which we can show various convergence speeds being free of the dimensionality θ . We give a brief review below for the readers' convenience.

3.1 A Class of Integral Probability Metrics (IPMs)

Firstly introduced in [25], the integral probability metric defines a metric on the space of probability measures $\mathcal{P}(E)$ based on a class of test functions.

Definition 3.1. Let Φ be a class of measurable functions on a Euclidean space E such that

$$\sup_{f \in \Phi} |f(x)| \leq C(1 + \|x\|),$$

for a constant $C > 0$ depending on Φ . Then for any $\mu, \mu' \in \mathcal{P}(E)$, the IPM D_Φ is defined by

$$D_\Phi(\mu, \mu') = \sup_{f \in \Phi} \left| \int_E f \, d(\mu - \mu') \right|.$$

Assumption 3.2 (Test function class). *Assume Φ satisfies the following properties:*

(a) *If μ is a signed measure on E ,*

$$\int_E f \, d\mu = 0, \quad \forall f \in \Phi \Rightarrow \mu \equiv 0;$$

(b) *There exists a constant $A > 0$, such that for any $f \in \Phi$, $\text{Lip}(f) \leq A$, $|f(0)| \leq A$, and for any $\mathcal{X} = \{x^1, \dots, x^N\} \subset E$, the empirical Rademacher complexity satisfies*

$$\text{Rad}_N(\Phi, \mathcal{X}) := \frac{1}{N} \mathbb{E} \sup_{f \in \Phi} \left| \sum_{i=1}^N \xi_i f(x^i) \right| \leq \frac{A}{N} \sqrt{\sum_{i=1}^N (\|x^i\|^2 + 1)},$$

where ξ_1, \dots, ξ_N are i.i.d. random variables drawn from the Rademacher distribution, i.e., $\mathbb{P}(\xi_i = 1) = \mathbb{P}(\xi_i = -1) = \frac{1}{2}$.

Then under Assumption 3.2, it is shown (cf. [25]) that the convergence rate of empirical measures associated from independent samples drawn from a given distribution $\mu \in \mathcal{P}^2(E)$, measured by D_Φ , is free of the dimensionality of E .

Theorem 3.3 ([25, Theorem 2.1]). *Under Assumption 3.2, D_Φ is a metric on $\mathcal{P}^1(E)$. For any μ_1 and $\mu_2 \in \mathcal{P}^1(E)$,*

$$D_\Phi(\mu_1, \mu_2) \leq A \mathcal{W}_1(\mu_1, \mu_2), \tag{14}$$

where \mathcal{W}_1 denotes the 1-Wasserstein metric. In addition, Given $\mu \in \mathcal{P}^2(E)$, let X^1, \dots, X^N be i.i.d. random variables drawn from the distribution μ and

$$\bar{\mu}^N = \frac{1}{N} \sum_{i=1}^N \delta_{X^i}$$

be the empirical measure of X^1, \dots, X^N . Then,

$$\begin{aligned} \mathbb{E} D_\Phi(\mu, \bar{\mu}^N) &\leq \frac{2A}{\sqrt{N}} \sqrt{\int_{\mathbb{R}^d} [\|x\|^2 + 1] \, d\mu(x)}, \\ \mathbb{E} [D_\Phi^2(\mu, \bar{\mu}^N)] &\leq \frac{5A^2}{N} \int_{\mathbb{R}^d} [\|x\|^2 + 1] \, d\mu(x). \end{aligned}$$

A similar result holds for measures on the space of continuous functions $C([0, T]; E)$ with additional assumptions regarding functions' modulus of continuity. Test function classes particularly discussed therein include the reproducing kernel Hilbert space (RKHS), the Barron space, and flow-induced function spaces [17]. Direct applications of metrics induced by such test function classes are that, the approximation error to the Nash equilibrium of finite player games by its mean-field limit is independent of the dimensionality of E , and that the empirical distribution associated with a finite-particle system to its McKean-Vlasov limit is free of CoD. While if measured by Wasserstein metric \mathcal{W}_1 or \mathcal{W}_2 , these convergence rates decrease as the dimension of E increases.

3.2 Numerical Analysis

Our analysis will focus on the following McKean-Vlasov FBSDEs for $(X_t, Y_t, Z_t) \in \mathbb{H}^2(\mathbb{R}^d \times \mathbb{R}^p \times \mathbb{R}^{p \times q})$:

$$\begin{cases} dX_t = b(t, X_t, m_1(t, X_t, \mathcal{L}(X_t))) dt + \sigma(t, X_t) dW_t, & X_0 = \xi, \\ dY_t = -h(t, \Theta_t, m_2(t, X_t, \mathcal{L}(X_t, Y_t))) dt + Z_t dW_t, & Y_T = g(X_T, m_3(X_T, \mathcal{L}(X_T))). \end{cases} \quad (15)$$

For the coupled McKean-Vlasov FBSDEs, that is, b depends on Y, Z or $\mathcal{L}(X, Y)$, similar results can be obtained under small duration conditions or the existence of global Lipschitz decoupling fields, like the situations in [24, 27, 43]. If m_1 and m_2 also depend on $\mathcal{L}(X, Y, Z)$, then we can also obtain the result following the method in [24, Section 4.2] if we have the following regularity [43] with respect to Z ,

$$\mathbb{E} \|Z_t - Z_{t'}\|_F^2 \leq C \|t - t'\|,$$

where $\|\cdot\|_F$ is the Frobenius norm.

Assumption 3.4. (a) The functions $b(t, x, m) : [0, T] \times \mathbb{R}^d \times \mathbb{R}^l \rightarrow \mathbb{R}^d$, $\sigma(t, x) : [0, T] \times \mathbb{R}^d \rightarrow \mathbb{R}^{d \times q}$, $h(t, x, y, z, m) : [0, T] \times \mathbb{R}^d \times \mathbb{R}^l \rightarrow \mathbb{R}^p$ and $g(x, m) : \mathbb{R}^d \times \mathbb{R}^l \rightarrow \mathbb{R}^p$ are Lipschitz with respect to x, y, z and m , with a Lipschitz constant L :

$$\begin{aligned} & \|b(t, x, m) - b(t, x', m')\|_F^2 + \|\sigma(t, x) - \sigma(t, x')\|_F^2 \\ & + \|h(t, x, y, z, m) - h(t, x', y', z', m')\|^2 + \|g(x, m) - g(x, m')\|^2 \\ & \leq L[\|x - x'\|^2 + \|y - y'\|^2 + \|z - z'\|_F^2 + \|m - m'\|^2]. \end{aligned}$$

(b) The functions $m_1(t, x, \mu) : [0, T] \times \mathbb{R}^d \times \mathcal{P}^2(\mathbb{R}^d) \rightarrow \mathbb{R}^l$, $m_2(t, x, \nu) : [0, T] \times \mathbb{R}^d \times \mathcal{P}^2(\mathbb{R}^d \times \mathbb{R}^p) \rightarrow \mathbb{R}^l$ and $m_3(x, \mu) : \mathbb{R}^d \times \mathcal{P}^2(\mathbb{R}^d) \rightarrow \mathbb{R}^l$ are Lipschitz with respect to x, μ and ν , with the same constant L :

$$\begin{aligned} & \|m_1(t, x, \mu) - m_1(t, x', \mu')\|^2 + \|m_2(t, x, \nu) - m_2(t, x', \nu')\|^2 \\ & + \|m_3(x, \mu) - m_3(x', \mu')\|^2 \leq L[\|x - x'\|^2 + D_{\Phi}^2(\mu, \mu') + D_{\Phi'}^2(\nu, \nu')], \end{aligned}$$

where $\Phi \subset \mathbb{R}^d$ and $\Phi' \subset \mathbb{R}^d \times \mathbb{R}^p$ are two classes of functions for the IPM and satisfy Assumption 3.2.

(c) The functions b, σ, h, g, m_1 and m_2 is $1/2$ -Hölder continuous with respect to t . We will use K to denote the Hölder constant.

(d) There exists a constant K , such that

$$\begin{aligned} & \|b(t, 0, 0)\|^2 + \|\sigma(t, 0)\|_F^2 + \|h(t, 0, 0)\|^2 + \|g(0, 0)\|^2 + \|m_1(t, 0, \delta_0)\|^2 \\ & \quad + \|m_2(t, 0, \delta_0)\|^2 + \|m_3(0, \delta_0)\|^2 + \mathbb{E}\|\xi\|^2 \leq K, \end{aligned}$$

where δ_0 denotes the Dirac measure at 0.

Lemma 3.5. Under Assumption 3.4, the MV-FBSDEs (15) possess a unique adapted solution (i.e., $(X_t, Y_t, Z_t) \in \mathbb{S}^2(\mathbb{R}^d) \times \mathbb{S}^2(\mathbb{R}^p) \times \mathbb{H}^2(\mathbb{R}^{p \times q})$) are adapted to the filtration $\mathbb{F} = (\mathcal{F}_t)_{t \in [0, T]}$ such that

$$\sup_{0 \leq t \leq T} [\mathbb{E}\|X_t\|^2 + \mathbb{E}\|Y_t\|^2] + \int_0^T \mathbb{E}\|Z_t\|_F^2 dt \leq C,$$

where $C > 0$ is a constant depending only on A, L, K and T .

Proof. Theorem 3.3 and Assumption 3.4 together imply that the MV-FBSDEs (15) satisfy the standard assumption in [11, Sections 4.2.1 and 4.2.2]. Therefore, with [11, Theorems 4.21 and 4.23], we obtain the desired result. \square

Since $\mathcal{L}(X_t, Y_t, Z_t)$ are deterministic functions of time t , we can view m_1 and m_2 in (15) as functions of (t, x) , and similarly view m_3 as a function of x . We define

$$\tilde{m}_1(t, x) = m_1(t, x, \mathcal{L}(X_t)), \quad \tilde{m}_2(t, x) = m_2(t, x, \mathcal{L}(X_t, Y_t)), \quad \tilde{m}_3(x) = m_3(x, \mathcal{L}(X_T)), \quad (16)$$

where (X_t, Y_t) is the solution to (15). This motivates us, in practice, to use neural networks to parameterize m_1, m_2 and m_3 with inputs of (t, x) and x , as stated in (6). To analyze the error associated with fictitious play, we define the following function sets \mathcal{M}_1 and \mathcal{M}_2 : given a fixed constant $M > 0$,

$$\begin{aligned} \mathcal{M}_1 &= \{m : [0, T] \times \mathbb{R}^d \rightarrow \mathbb{R}^l, \|m(t, x) - m(t', x')\|^2 \leq M[|t - t'| + \|x - x'\|^2], \\ & \quad \|m(t, x)\| \leq M[1 + \|x\|]\}, \\ \mathcal{M}_2 &= \{m : \mathbb{R}^d \rightarrow \mathbb{R}^l, \|m(x) - m(x')\|^2 \leq M\|x - x'\|^2, \|m(x)\| \leq M[1 + \|x\|]\}. \end{aligned}$$

Let $\mathcal{M} = \mathcal{M}_1 \times \mathcal{M}_1 \times \mathcal{M}_2$. We then define a map $\mathcal{T} : \mathcal{M} \rightarrow C([0, T] \times \mathbb{R}^d) \times C([0, T] \times \mathbb{R}^d) \times C(\mathbb{R}^d)$ such that, for any $(\bar{m}_1, \bar{m}_2, \bar{m}_3) \in \mathcal{M}$:

$$\mathcal{T}(\bar{m}_1, \bar{m}_2, \bar{m}_3)(t, x) := (m_1(t, x, \mathcal{L}(\bar{X}_t)), m_2(t, x, \mathcal{L}(\bar{X}_t, \bar{Y}_t)), m_3(x, \mathcal{L}(\bar{X}_T))),$$

where $(\bar{X}_t, \bar{Y}_t, \bar{Z}_t)$ is the solution to the decoupled FBSDEs:

$$\begin{cases} d\bar{X}_t = b(t, \bar{X}_t, \bar{m}_1(t, \bar{X}_t)) dt + \sigma(t, \bar{X}_t) dW_t, & \bar{X}_0 = \xi, \\ d\bar{Y}_t = -h(t, \bar{\Theta}_t, \bar{m}_2(t, \bar{X}_t)) dt + \bar{Z}_t dW_t, & \bar{Y}_T = g(\bar{X}_T, m_3(\bar{X}_T)). \end{cases} \quad (17)$$

That is, \mathcal{T} maps any element in \mathcal{M} to the functions $(m_1(t, x, \cdot), m_2(t, x, \cdot), m_3(x, \cdot))$ with \cdot being the law of the FBSDE system (17). This definition corresponds to the idea of fictitious play that sequentially updates the quantity $Q^{(k)}$ of interest.

The next lemma shows that if M is large enough, then \mathcal{T} is closed in \mathcal{M} .

Lemma 3.6. There exists a constant $M_0 > 0$, depending only on A, L, K and T , such that for any $M \geq M_0$, $\mathcal{T}m \in \mathcal{M}$ for any $m \in \mathcal{M}$.

Proof. Notice that as long as $M \geq L$, the Lipschitz continuity with respect to x is always kept. By the definition of \mathcal{T} , Assumption 3.4(c) and inequality (14), in order to show the Hölder continuity of $(\mathcal{T}m_1, \mathcal{T}m_2)$ with respect to t , it suffices to prove that

$$\mathbb{E}\|\bar{X}_t - \bar{X}_{t'}\|^2 + \mathbb{E}\|\bar{Y}_t - \bar{Y}_{t'}\|^2 \leq C\|t - t'\|,$$

which can be obtained by [49, Theorem 5.2.2]. Here C is a positive constant only depending on A, L, K, T .

The linear growth property with respect to x can be obtained using a similar method as in [5, Section 4] and we hence omit the proof. \square

The next result focuses on how error changes in terms of the stage of fictitious play. Suppose we have a sequence of functions $(m_1^k, m_2^k, m_3^k) \in \mathcal{M}$, $k \in \mathbb{N}$. For each k , let $(X_t^k, Y_t^k, Z_t^k) \in \mathbb{H}^2(\mathbb{R}^d \times \mathbb{R}^p \times \mathbb{R}^{p \times q})$ solves

$$\begin{cases} dX_t^k = b(t, X_t^k, m_1^k(t, X_t^k)) dt + \sigma(t, X_t^k) dW_t, & X_0^k = \xi, \\ dY_t^k = -h(t, \Theta_t^k, m_2^k(t, X_t^k)) dt + Z_t^k dW_t, & Y_T^k = g(X_T^k, m_3^k(X_T^k)). \end{cases} \quad (18)$$

The theorem below shows how m_i^{k+1} and m_i^k , $i = 1, 2, 3$, should be related in order to achieve small errors. More discussions will be given after the proof.

Theorem 3.7. *Under Assumptions 3.2 and 3.4, there exist constants $C > 0$ and $0 < q < 1$ which only depend on A, L, K, T and M , such that*

$$\begin{aligned} & \sup_{0 \leq t \leq T} [\mathbb{E}\|X_t - X_t^k\|^2 + \mathbb{E}\|Y_t - Y_t^k\|^2] + \int_0^T \mathbb{E}\|Z_t - Z_t^k\|_F^2 dt \\ & \leq C \left\{ q^k + \sum_{j=0}^{k-1} q^{k-j} \left[\int_0^T \mathbb{E}\|(m_1^{j+1}, m_2^{j+1})(t, X_t^{j+1}) - (\tilde{m}_1^j, \tilde{m}_2^j)(t, X_t^{j+1})\|^2 dt \right. \right. \\ & \quad \left. \left. + \mathbb{E}\|m_3^{j+1}(X_T^{j+1}) - \tilde{m}_3^j(X_T^{j+1})\|^2 \right] \right\}, \quad (19) \end{aligned}$$

where (X_t, Y_t, Z_t) solves the MV-FBSDEs (15), (X_t^k, Y_t^k, Z_t^k) solves (18), and $(\tilde{m}_1^k, \tilde{m}_2^k, \tilde{m}_3^k) := \mathcal{T}(m_1^k, m_2^k, m_3^k)$.

Proof. In the sequel, we will use C to denote a positive constant depending only on A, L, K, T and M , which may vary from line to line.

We then estimate the differences between Θ and Θ^k . Recall $\tilde{m}_1, \tilde{m}_2, \tilde{m}_3$ from (16), for any given $k \geq 1$, we define $\delta X_t^k = X_t - X_t^k$, $\delta Y_t^k = Y_t - Y_t^k$, $\delta Z_t^k = Z_t - Z_t^k$, and

$$\begin{aligned} I_1^k &= \int_0^T \mathbb{E}\|m_1^k(t, X_t^k) - \tilde{m}_1^{k-1}(t, X_t^k)\|^2 dt, \\ I_2^k &= \int_0^T \mathbb{E}\|m_2^k(t, X_t^k) - \tilde{m}_2^{k-1}(t, X_t^k)\|^2 dt, \\ I_3^k &= \mathbb{E}\|m_3^k(X_T^k) - \tilde{m}_3^{k-1}(X_T^k)\|^2, \\ \delta h_t &= h(t, \Theta_t, \tilde{m}_2(t, X_t)) - h(t, \Theta_t^k, m_2^k(t, X_t^k)). \end{aligned}$$

Combining (15), (18) and [49, Theorem 3.2.4], we know that for any $t \in [0, T]$:

$$\begin{aligned}
\sup_{0 \leq s \leq t} \mathbb{E} \|\delta X_s^k\|^2 &\leq C \int_0^t \mathbb{E} \|b(s, X_s^k, \tilde{m}_1(s, X_s^k)) - b(s, X_s^k, m_1^k(s, X_s^k))\|^2 ds \\
&\leq C \int_0^t \mathbb{E} \|\tilde{m}_1(s, X_s^k) - m_1^k(s, X_s^k)\|^2 ds \\
&\leq C \int_0^t \mathbb{E} \|\tilde{m}_1(s, X_s^k) - \tilde{m}_1^{k-1}(s, X_s^k)\|^2 ds + CI_1^k \\
&= C \int_0^t \mathbb{E} \|m_1(s, X_s^k, \mathcal{L}(X_s)) - m_1(s, X_s^k, \mathcal{L}(X_s^{k-1}))\|^2 ds + CI_1^k \\
&\leq C \int_0^t \mathbb{E} D_{\Phi}^2(\mathcal{L}(X_s), \mathcal{L}(X_s^{k-1})) ds + CI_1^k \\
&\leq C \int_0^t \mathbb{E} \|\delta X_s^{k-1}\|^2 ds + CI_1^k.
\end{aligned} \tag{20}$$

Then by induction, one has

$$\int_0^t \mathbb{E} \|\delta X_s^k\|^2 ds \leq \frac{C^k}{k!} \int_0^t (t-s)^k \mathbb{E} \|\delta X_s^0\|^2 ds + \sum_{j=1}^k \frac{(Cj)^k}{j!} I_1^{k+1-j}. \tag{21}$$

Noticing that with $m_1^0 \in \mathcal{M}_1$, [49, Theorem 3.2.2] gives

$$\sup_{0 \leq t \leq T} \mathbb{E} \|X_t^0\|^2 \leq C.$$

Combining it with Lemma 3.5 and the estimate (21) yields

$$\int_0^T \mathbb{E} \|\delta X_t^k\|^2 dt \leq \frac{(CT)^k}{k!} + \sum_{j=1}^k \frac{(CT)^j}{j!} I_1^{k+1-j}.$$

Noticing that there exists another constant $\tilde{C} > 0$ and $0 < q < 1$ such that

$$\frac{(CT)^k}{k!} \leq \tilde{C}q^k, \quad \forall k \in \mathbb{N}^+,$$

therefore

$$\int_0^T \mathbb{E} \|\delta X_t^k\|^2 dt \leq Cq^k + C \sum_{j=0}^{k-1} q^{k-j} I_1^{j+1}.$$

Plugging the above inequality into (20) produces the X -part in (19). The analysis for (Y, Z) -part can be obtained in a similar way if one replaces [49, Theorems 3.2.2 and 3.2.4] in the above proof for X -part by [49, Theorem 4.2.1 and 4.2.3] for (Y, Z) -part. \square

If we want to apply Theorem 3.7 to explain the convergence of Deep MV-FBSDE Algorithm, one issue is that in the right side of inequality (19) X_t^{j+1} occurs while in the optimization problems (6) X_t^j occurs. The following lemma shows the legitimacy of replacing X_t^{j+1} by X_t^j .

Lemma 3.8. *Assume that*

$$\|\sigma(t, x)\|_S \leq K, \quad \|\phi(t, x, m)\|_\infty \leq K,$$

where $\|\cdot\|_S$ denotes the spectral norm on $\mathbb{R}^{d \times q}$, $\|\cdot\|_\infty$ denotes the infinity norm on \mathbb{R}^q , and ϕ satisfies that

$$b(t, x, m) = \sigma(t, x)\phi(t, x, m).$$

Let \bar{m}^1, \bar{m}^2 be two arbitrary functions in \mathcal{M}_1 , and \bar{X}^1 and \bar{X}^2 be the associated solutions to the SDEs:

$$d\bar{X}_t^i = b(t, \bar{X}_t^i, \bar{m}^i(t, \bar{X}_t^i)) dt + \sigma(t, \bar{X}_t^i) dW_t, \quad \bar{X}_0^i = \xi, \quad i = 1, 2.$$

Let $m, m' \in \mathcal{M}_2$, then for any $\epsilon \in (0, 1)$, there exists a constant $C(\epsilon)$, which only depends on A, L, K, T, M and ϵ such that

$$\mathbb{E}\|m(\bar{X}_t^1) - m'(\bar{X}_t^1)\|^2 \leq C(\epsilon) [\mathbb{E}\|m(\bar{X}_t^2) - m'(\bar{X}_t^2)\|^2]^\epsilon, \quad \forall t \in [0, T].$$

Proof. The proof of this lemma is based on the Girsanov theorem; See, e.g., [24, Theorem 4]. \square

We are now ready to justify the Deep MV-FBSDE Algorithm. Here we take the version using the Deep BSDE solver as an instance. Similar results can also be established for the version using the DBDP solver.

We take a sequence $\{\hat{m}_1^k, \hat{m}_2^k, \hat{m}_3^k\}_{k \in \mathbb{N}} \in \mathcal{M}$, in which M is large enough such that the closeness of \mathcal{T} in Lemma 3.6 holds. Note that here \hat{m}_i^k are general functions, and can be, but not limited to, the functions \hat{m}_i^k defined in **Step 2** of Section 2.1. Recall the notations of partition π on the interval $[0, T]$ of size N_T : $0 = t_0 < t_1 < \dots < t_i < \dots < t_{N_T}$ with $\Delta t_i = t_{i+1} - t_i$ and $\Delta W_{t_i} = W_{t_{i+1}} - W_{t_i}$. Let $\{(u^k, v_i^k)\}_{k \in \mathbb{N}, 0 \leq i \leq N_T - 1}$ be a sequence of functions such that $u^k \in C(\mathbb{R}^d; \mathbb{R}^p)$ and $v_i^k \in C(\mathbb{R}^d; \mathbb{R}^{p \times q})$ for any $k \in \mathbb{N}$ and $0 \leq i \leq N_T - 1$, we define

$$\begin{cases} \tilde{X}_{t_{i+1}}^{k, \pi} = \tilde{X}_{t_i}^{k, \pi} + b(t_i, \tilde{X}_{t_i}^{k, \pi}, \hat{m}_1^k(t_i, \tilde{X}_{t_i}^{k, \pi}))\Delta t_i + \sigma(t_i, \tilde{X}_{t_i}^{k, \pi})\Delta W_{t_i}, \\ \tilde{Y}_{t_{i+1}}^{k, \pi} = \tilde{Y}_{t_i}^{k, \pi} - h(t_i, \tilde{\Theta}_{t_i}^{k, \pi}, \hat{m}_2^k(t_i, \tilde{X}_{t_i}^{k, \pi}))\Delta t_i + v_i^k(\tilde{X}_{t_i}^{k, \pi})\Delta W_{t_i}, \end{cases}$$

with initial conditions $\tilde{X}_0^{k, \pi} = \xi$ and $\tilde{Y}_0^{k, \pi} = u^k(\tilde{X}_0^{k, \pi})$. The next theorem gives the convergence of the Deep MV-FBSDE Algorithm with the Deep BSDE solver.

Theorem 3.9. *Under Assumptions 3.2 and 3.4, for any $\epsilon \in (0, 1)$, there exist a constant $q \in (0, 1)$ which only depend on A, L, K, T and M and $C(\epsilon) > 0$ which depend on A, L, K, T, M and ϵ , such*

that

$$\begin{aligned}
& \sup_{0 \leq t \leq T} [\mathbb{E} \|X_t - \tilde{X}_{\pi(t)}^{k,\pi}\|^2 + \mathbb{E} \|Y_t - \tilde{Y}_{\pi(t)}^{k,\pi}\|^2] + \int_0^T \mathbb{E} \|Z_t - v_t^k(\tilde{X}_{\pi(t)}^{k,\pi})\|_F^2 dt \\
& \leq C(\epsilon) \left\{ q^k + \|\pi\| + \frac{1}{N} + \mathbb{E} \|\tilde{Y}_T^{k,\pi} - g(\tilde{X}_T^{k,\pi}, \hat{m}_3^k(\tilde{X}_T^{k,\pi}))\|^2 \right. \\
& \quad + \sum_{j=0}^{k-1} q^{k-j} \mathbb{E} \|\tilde{Y}_T^{j,\pi} - g(\tilde{X}_T^{j,\pi}, \hat{m}_3^j(\tilde{X}_T^{j,\pi}))\|^2 \\
& \quad + \sum_{j=0}^{k-1} q^{k-j} \left[\mathbb{E} \|\hat{m}_3^{j+1}(\tilde{X}_T^{j,\pi}) - m_3(\tilde{X}_T^{j,\pi}, \mu_T^j)\|^2 \right. \\
& \quad + \sum_{i=0}^{N_T-1} q^{k-j} \mathbb{E} \|\hat{m}_1^{j+1}(t_i, \tilde{X}_{t_i}^{j,\pi}) - m_1(t_i, \tilde{X}_{t_i}^{j,\pi}, \mu_{t_i}^j)\|^2 \Delta t_i \Big] \\
& \quad \left. + \sum_{i=0}^{N_T-1} q^{k-j} \mathbb{E} \|\hat{m}_2^{j+1}(t_i, \tilde{X}_{t_i}^{j,\pi}) - m_2(t_i, \tilde{X}_{t_i}^{j,\pi}, \nu_{t_i}^j)\|^2 \Delta t_i \right\}^\epsilon, \tag{22}
\end{aligned}$$

in which $\|\pi\| := \max_{0 \leq i \leq N_T-1} (t_{i+1} - t_i)$, $\pi(t) = t_i$ if $t \in [t_i, t_{i+1})$ and $\{\mu_{t_i}^k\}_{i=0}^{N_T}$ and $\{\nu_{t_i}^k\}_{i=0}^{N_T}$ are defined as the empirical distribution of $\tilde{X}_{t_i}^{k,\pi}$ and $(\tilde{X}_{t_i}^{k,\pi}, \tilde{Y}_{t_i}^{k,\pi})$:

$$\mu_{t_i}^k = \frac{1}{N} \sum_{n=1}^N \delta_{\tilde{X}_{t_i}^{k,\pi,n}}, \quad \nu_{t_i}^k = \frac{1}{N} \sum_{n=1}^N \delta_{(\tilde{X}_{t_i}^{k,\pi,n}, \tilde{Y}_{t_i}^{k,\pi,n})},$$

where

$$\begin{aligned}
\tilde{X}_{t_{i+1}}^{k,\pi,n} &= \tilde{X}_{t_i}^{k,\pi,n} + b(t_i, \tilde{X}_{t_i}^{k,\pi,n}, \hat{m}_1^k(t_i, \tilde{X}_{t_i}^{k,\pi,n})) \Delta t_i + \sigma(t_i, \tilde{X}_{t_i}^{k,\pi,n}) \Delta W_{t_i}^n, \quad \tilde{X}_0^{k,\pi,n} = \xi^n, \\
\tilde{Y}_{t_{i+1}}^{k,\pi,n} &= \tilde{Y}_{t_i}^{k,\pi,n} - h(t_i, \tilde{\Theta}_{t_i}^{k,\pi,n}, \hat{m}_2^k(t_i, \tilde{X}_{t_i}^{k,\pi,n})) \Delta t_i + v_i^k(\tilde{X}_{t_i}^{k,\pi,n}) \Delta W_{t_i}^n, \quad \tilde{Y}_0^{k,\pi,n} = u^k(\xi^n),
\end{aligned}$$

$\{W_t^n\}_{n=1}^N$ are i.i.d. Brownian motion in \mathbb{R}^q and $\{\xi^n\}_{n=1}^N$ are i.i.d. copies of ξ .

Let $(\tilde{X}_t^k, \tilde{Y}_t^k, \tilde{Z}_t^k)$ be the solution of

$$\begin{cases} d\tilde{X}_t^k = b(t, \tilde{X}_t^k, \hat{m}_1^k(t, \tilde{X}_t^k)) dt + \sigma(t, \tilde{X}_t^k) dW_t, & \tilde{X}_0^k = \xi, \\ d\tilde{Y}_t^k = -h(t, \tilde{\Theta}_t^k, \hat{m}_2^k(t, \tilde{X}_t^k)) dt + \tilde{Z}_t^k dW_t, & \tilde{Y}_T^k = g(\tilde{X}_T^k, \hat{m}_3^k(\tilde{X}_T^k)), \end{cases}$$

\mathcal{N}' and $\{\mathcal{N}_i\}_{i=0}^{N_T-1}$ be any subsets of $C(\mathbb{R}^d; \mathbb{R}^p)$ and $C(\mathbb{R}^d; \mathbb{R}^{p \times q})$, respectively. Then, for any $k \in \mathbb{N}$,

$$\begin{aligned}
& \inf_{u^k \in \mathcal{N}', v_i^k \in \mathcal{N}_i} \mathbb{E} \|\tilde{Y}_T^{k,\pi} - g(\tilde{X}_T^{k,\pi}, \hat{m}_3^k(\tilde{X}_T^{k,\pi}))\|^2 \\
& \leq C \left\{ \|\pi\| + \inf_{u^k \in \mathcal{N}'} \mathbb{E} \|\tilde{Y}_0^k - u^k(\tilde{X}_0^{k,\pi})\|^2 + \sum_{i=0}^{N_T-1} \inf_{v_i^k \in \mathcal{N}_i} \mathbb{E} \|\tilde{Z}_{t_i}^{k,\pi} - v_i^k(\tilde{X}_{t_i}^{k,\pi})\|^2 \right\}, \tag{23}
\end{aligned}$$

where $\tilde{Z}_{t_i}^{k,\pi} = (\Delta t_i)^{-1} \mathbb{E} [\int_{t_i}^{t_{i+1}} \tilde{Z}_t^k dt | \tilde{X}_{t_i}^{k,\pi}]$.

Finally, for any $k \in \mathbb{N}$,

$$\begin{aligned}
& \inf_{(\hat{m}_1^k, \hat{m}_2^k, \hat{m}_3^k) \in \mathcal{M}} \left\{ \sum_{i=0}^{N_T-1} \mathbb{E} \|\hat{m}_1^{k+1}(t_i, \tilde{X}_{t_i}^{k,\pi}) - m_1(t_i, \tilde{X}_{t_i}^{k,\pi}, \mu_{t_i}^k)\|^2 \Delta t_i \right. \\
& \quad + \sum_{i=0}^{N_T-1} \mathbb{E} \|\hat{m}_2^{k+1}(t_i, \tilde{X}_{t_i}^{k,\pi}) - m_2(t_i, \tilde{X}_{t_i}^{k,\pi}, \nu_{t_i}^k)\|^2 \Delta t_i \\
& \quad \left. + \mathbb{E} \|\hat{m}_3^{k+1}(\tilde{X}_T^{k,\pi}) - m_3(\tilde{X}_T^{k,\pi}, \mu_T^k)\|^2 \right\} \\
& \leq C \left[\frac{1}{N} + \|\pi\| + \mathbb{E} \|\tilde{Y}_T^{k,\pi} - g(\tilde{X}_T^{k,\pi}, \hat{m}_3^k(\tilde{X}_T^{k,\pi}))\|^2 \right]. \tag{24}
\end{aligned}$$

Proof. Combining Assumptions 3.2 and 3.4, the fact that $(\hat{m}_1^k, \hat{m}_2^k, \hat{m}_3^k) \in \mathcal{M}$ and [27, Theorem 1 and 2], we obtain (23) and

$$\begin{aligned}
& \sup_{0 \leq t \leq T} [\mathbb{E} \|\tilde{X}_t^k - \tilde{X}_{\pi(t)}^{k,\pi}\|^2 + \mathbb{E} \|\tilde{Y}_t^k - \tilde{Y}_{\pi(t)}^{k,\pi}\|^2] + \int_0^T \mathbb{E} \|\tilde{Z}_t^k - v_i^k(\tilde{X}_{\pi(t)}^{k,\pi})\|_F^2 dt \\
& \leq C [\|\pi\| + \mathbb{E} \|\tilde{Y}_T^{k,\pi} - g(\tilde{X}_T^{k,\pi}, \hat{m}_3^k(\tilde{X}_T^{k,\pi}))\|^2]. \tag{25}
\end{aligned}$$

Applying Theorem 3.7 to $(\tilde{X}_t^k, \tilde{Y}_t^k, \tilde{Z}_t^k)$, we have

$$\begin{aligned}
& \sup_{0 \leq t \leq T} [\mathbb{E} \|X_t - \tilde{X}_t^k\|^2 + \mathbb{E} \|Y_t - \tilde{Y}_t^k\|^2] + \int_0^T \mathbb{E} \|Z_t - \tilde{Z}_t^k\|_F^2 dt \\
& \leq C \left\{ q^k + \sum_{j=0}^{k-1} q^{k-j} \left[\int_0^T \left(\mathbb{E} \|\hat{m}_1^{j+1}(t, \tilde{X}_t^{j+1}) - m_1(t, \tilde{X}_t^{j+1}, \mathcal{L}(\tilde{X}_t^j))\|^2 \right. \right. \right. \\
& \quad \left. \left. + \mathbb{E} \|\hat{m}_2^{j+1}(t, \tilde{X}_t^{j+1}) - m_2(t, \tilde{X}_t^{j+1}, \mathcal{L}(\tilde{X}_t^j, \tilde{Y}_t^j))\|^2 \right) dt \right. \\
& \quad \left. \left. + \mathbb{E} \|\hat{m}_3^{j+1}(\tilde{X}_T^{j+1}) - m_3(\tilde{X}_T^{j+1}, \mathcal{L}(\tilde{X}_T^j))\|^2 \right] \right\}.
\end{aligned}$$

Using Theorem 3.6, we know that

$$(m_1(t, x, \mathcal{L}(\tilde{X}_t^k)), m_2(t, x, \mathcal{L}(\tilde{X}_t^k, \tilde{Y}_t^k)), m_3(x, \mathcal{L}(\tilde{X}_T^k))) \in \mathcal{M}. \tag{26}$$

Then Lemma 3.8 gives that

$$\begin{aligned}
& \sup_{0 \leq t \leq T} [\mathbb{E} \|X_t - \tilde{X}_t^k\|^2 + \mathbb{E} \|Y_t - \tilde{Y}_t^k\|^2] + \int_0^T \mathbb{E} \|Z_t - \tilde{Z}_t^k\|_F^2 dt \\
& \leq C \left\{ q^k + \sum_{j=0}^{k-1} q^{k-j} \left[\int_0^T \left(\mathbb{E} \|\hat{m}_1^{j+1}(t, \tilde{X}_t^j) - m_1(t, \tilde{X}_t^j, \mathcal{L}(\tilde{X}_t^j))\|^2 \right. \right. \right. \\
& \quad \left. \left. + \mathbb{E} \|\hat{m}_2^{j+1}(t, \tilde{X}_t^j) - m_2(t, \tilde{X}_t^j, \mathcal{L}(\tilde{X}_t^j, \tilde{Y}_t^j))\|^2 \right) dt \right. \\
& \quad \left. \left. + \mathbb{E} \|\hat{m}_3^j(\tilde{X}_T^j) - m_3(\tilde{X}_T^j, \mathcal{L}(\tilde{X}_T^j))\|^2 \right] \right\}^c. \tag{27}
\end{aligned}$$

Combining with inequality (25) and Theorem 3.3, we know that for any $k \in \mathbb{N}$,

$$\begin{aligned}
& \mathbb{E} D_{\Phi}^2(\mathcal{L}(X_t^k), \mu_{\pi(t)}^k) + \mathbb{E} D_{\Phi'}^2(\mathcal{L}(X_t^k, Y_t^k), \nu_{\pi(t)}^k) \\
& \leq C \left[\|\pi\| + \frac{1}{N} + \mathbb{E} \|\tilde{Y}_T^{k,\pi} - g(\tilde{X}_T^{k,\pi}, \hat{m}_3^k(\tilde{X}_T^{k,\pi}))\|^2 \right]. \tag{28}
\end{aligned}$$

Combining the last inequality with inequalities (25) and (27), we have deduced inequality (22).

Finally, we prove the inequality (24). Recalling (26), it suffices to show

$$\begin{aligned} & \sum_{i=0}^{N_T-1} \left(\mathbb{E} \|m_1(t_i, \tilde{X}_{t_i}^{k,\pi}, \mathcal{L}(\tilde{X}_{t_i}^k)) - m_1(t_i, \tilde{X}_{t_i}^{k,\pi}, \mu_{t_i}^k)\|^2 \right. \\ & \quad \left. + \mathbb{E} \|m_2(t_i, \tilde{X}_{t_i}^{k,\pi}, \mathcal{L}(\tilde{X}_{t_i}^k, \tilde{Y}_{t_i}^k)) - m_1(t_i, \tilde{X}_{t_i}^{k,\pi}, \nu_{t_i}^k)\|^2 \right) \Delta t_i \\ & + \mathbb{E} \|m_3(\tilde{X}_T^{k,\pi}, \mathcal{L}(\tilde{X}_T^k)) - m_3(\tilde{X}_T^{k,\pi}, \mu_T^k)\|^2 \\ & \leq C \left[\frac{1}{N} + \|\pi\| + \mathbb{E} \|\tilde{Y}_T^{k,\pi} - g(\tilde{X}_T^{k,\pi}, \hat{m}_3^k(\tilde{X}_T^{k,\pi}))\|^2 \right], \end{aligned}$$

which follows inequality (28). Thus we've obtained inequality (24). \square

Theorem 3.9 shows that if we further require $(\mathbf{m}_1, \mathbf{m}_2, \mathbf{m}_3) \in \mathcal{M}$ in the optimization problems (6), the Deep MV-FBSDE algorithm will converge. Specifically, the inequality (22) shows that the distance between the true solution of the MV-FBSDE (15) and the output of the Deep MV-FBSDE algorithm can be controlled by the mesh size, the number of samples to approximate the distribution, the loss functions for the supervised learning problems (6) and the Deep BSDE method (9) at all the previous stages and an exponential decay term with respect to the number of iterations. Inequality (23) is a direct application of Theorem 2 in [27], which shows that the loss function of the Deep BSDE method at each stage can be small if the approximation capacity of the parametric function spaces (\mathcal{N}' and $\{\mathcal{N}_i\}_{i=0}^{N_T-1}$) is large. Finally, inequality (24) shows that the loss function for the supervised learning can be small if the loss function of the Deep BSDE method at the last stage is small. In practice, to ensure that the optimized neural networks $\mathbf{m}_1, \mathbf{m}_2, \mathbf{m}_3$ satisfy the Lipschitz constraints, we can use the method in [19] to obtain an efficient and accurate estimation of Lipschitz constants for neural networks. If needed, we can also use various techniques proposed in recent literature (see, *e.g.*, [3, 22, 20, 19, 41]) to regularize the Lipschitz constants during the optimization.

4 Numerical Results

The algorithm is implemented in Python using the machine learning library TensorFlow. The code can be found in the public GitHub repository³, and thus the results presented here can be straightforwardly reproduced and further developed.

4.1 A Benchmark Example with Explicit Solution

We first consider the following MV-FBSDEs for (X_t, Y_t, Z_t) :

$$\begin{cases} dX_t^i = \left[\sin(\tilde{\mathbb{E}}_{x_t' \sim \mu_t} e^{-\frac{\|x_t - x_t'\|^2}{d}} - e^{-\frac{\|x_t\|^2}{d+2t}} \left(\frac{d}{d+2t} \right)^{\frac{d}{2}} \right) + \frac{1}{2}(m_t^Y - \sin(t)e^{-\frac{t}{2}}) \right] dt + dW_t^i, \\ dY_t = \left[\frac{Z_t^1 + \dots + Z_t^d}{\sqrt{d}} - \frac{Y_t}{2} + \sqrt{Y_t^2 + \|Z_t\|^2 + 1} - \sqrt{2} \right] dt + Z_t dW_t, \end{cases} \quad (29)$$

with initial and terminal conditions $X_0^i = 0$ and $Y_T = \sin\left(T + \frac{X_T^1 + \dots + X_T^d}{\sqrt{d}}\right)$, where X_t^i denotes the i^{th} entry of the d -dimensional forward process X_t , $\mu_t = \mathcal{L}(X_t)$, $m_t^Y = \mathbb{E}[Y_t]$, $p = 1$ and $q = d$. The

³<https://github.com/frankhan91/DeepMVBSDE>

expectation $\tilde{\mathbb{E}}$ is with respect to $x'_t \sim \mu_t$ only. It can be verified straightforwardly that

$$X_t = W_t, \quad Y_t = \sin\left(t + \frac{X_t^1 + \dots + X_t^d}{\sqrt{d}}\right), \quad Z_t^i = \frac{1}{\sqrt{d}} \cos\left(t + \frac{X_t^1 + \dots + X_t^d}{\sqrt{d}}\right),$$

is the solution of the above MV-FBSDEs. Here the distribution-dependent functions are defined as

$$m_1(t, x, \mathcal{L}(\Theta_t)) = \tilde{\mathbb{E}}_{x' \sim \mathcal{L}(X_t)} e^{-\frac{\|x-x'\|^2}{d}} + \frac{1}{2} m_t^Y, \\ m_2 \equiv 0, \quad m_3 \equiv 0.$$

We first apply the proposed Deep MV-FBSDE algorithm to solve this problem when the dimension d equals 5 and 10, and $T = 0.5$. We have tested both the Deep BSDE solver and the DBDP solver for this problem. We discretize the time interval into 20 equal subintervals and simulate $N = 1500$ SDE paths to approximate the state distribution $\mathcal{L}(\Theta_t)$. The fictitious play is run for 30 stages in total. We use feedforward neural networks with two hidden layers of width 24 and Rectified Linear Unit (ReLU) activation function to approximate the unknown functions in the BSDE solver and m_1 when approximating the distribution dependence.

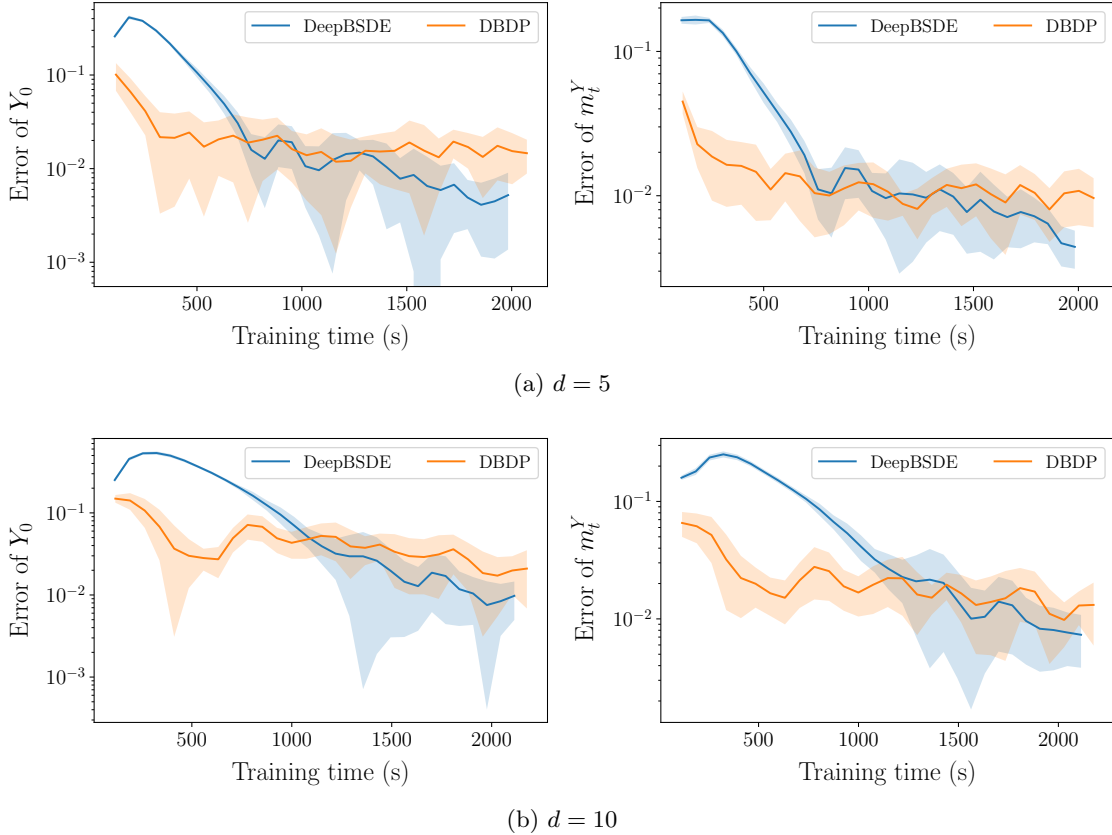


Figure 1: The absolute error of Y_0 (left) and L^2 error of m_t^Y (right) for equation (29) along the training process, in the case of $d = 5$ (top) and $d = 10$ (bottom). The shaded area depicts the mean \pm the standard deviation computed from 5 independent runs.

The training curves of absolute error of Y_0 and L^2 error of m_t^Y versus training time (implemented on a Macbook Pro with a 2.40 Gigahertz Intel Core i9 processor) are shown in Figure 1. Using

the Deep BSDE method, the algorithm finally finds the solution whose absolute error of Y_0 and L^2 error of m_t^Y are 0.54% and 0.43% when $d = 5$ and 1.01% and 0.80% when $d = 10$, respectively. Using the DBDP method, the algorithm finally finds the solution whose absolute error of Y_0 and L^2 error of m_t^Y are 1.60% and 0.92% when $d = 5$ and 1.75% and 1.09% when $d = 10$, respectively. The results corroborate our convergence analysis that the proposed algorithm can find accurate solutions in high dimensions with either BSDE solver. From Figure 1 and the final accuracy, we can see that the Deep BSDE solver performs slightly better than the DBDP solver when applied to this problem, consistent with the results reported in [21].

We further investigate the numerical error of the Deep MV-FBSDE algorithm with varying dimensions d , using the Deep BSDE method as a representative BSDE solver. The dimensions considered are $d = 5, 8, 10, 12, 15$. Two important parameters are increased linearly with d . Specifically, the number of SDE paths N is set at (500, 800, 1000, 1200, 1500) for the corresponding values of d , and the network widths are set at (12, 18, 24, 30, 36), respectively. In contrast, other settings are kept constant across dimensions: our network architecture consists of feedforward neural networks with two hidden layers and a ReLU activation function, the number of fictitious stages remains fixed at 80, and the learning rate schedule is unchanged. Figure 2 (the left panel) illustrates the error bars (computed from 5 independent runs) for the final error of Y_0 across different dimensions. For the problem (29), as the dimension increases from 5 to 15, we maintain an approximate solution for Y_0 with an absolute error below 2%. This is accomplished with a reasonably modest increase in computational cost. Figure 2 (the right panel) depicts the evolution of the error during fictitious play. As expected, convergence requires more fictitious plays as the dimension increases, but the increase is not dramatic. These results suggest that the proposed Deep MV-FBSDE algorithm exhibits favorable scaling with respect to problem dimensions, standing in stark contrast to traditional numerical methods that are susceptible to the curse of dimensionality.

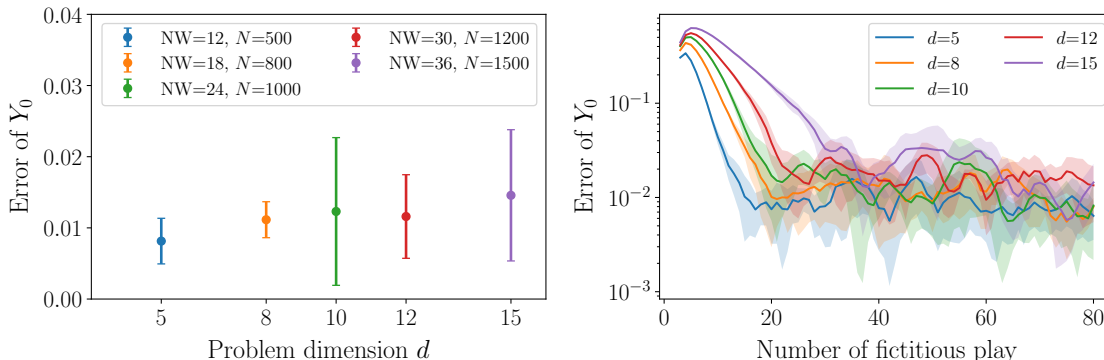


Figure 2: The absolute error of Y_0 in solving equation (29) using the Deep BSDE method across different dimensions $d = (5, 8, 10, 12, 15)$. The network width (NW) and the number of particles N increase linearly as d increases. The left panel shows error bars for the final errors, while the right panel portrays the error evolution during fictitious play. The shaded area depicts the mean \pm the standard deviation computed from 5 independent runs.

4.2 A Mean-field Game of Cucker-Smale Flocking Model

In this subsection, we consider a mean-field problem of Cucker-Smale [14] flocking model motivated from [39, 40]. The Cucker-Smale model plays an important role in modeling and analyzing the flocking behaviors, which refers to the collective motion by a group of self-propelled entities such as

birds, fish, bacteria, and insects. When the number of entities is very large, it is natural to consider the mean-field limit system. Below, we consider a mean-field game version of the Cucker-Smale model where every agent chooses her acceleration to minimize the cost of acceleration and their location and velocity misalignments.

We model a representative agent's dynamics by

$$\begin{cases} dx_t = v_t dt, \\ dv_t = u_t dt + C dW_t, \end{cases}$$

where $x_t \in \mathbb{R}^n$ and $v_t \in \mathbb{R}^n$ are time- t position and velocity vectors of the agent, $u_t \in \mathbb{R}^n$ is the acceleration control input, and W is a p -dimensional Brownian motion. The agent aims to minimize

$$\mathbb{E} \int_0^T \|u_t\|_R^2 + \mathcal{C}(x_t, v_t; f_t) dt, \quad (30)$$

over possible u_t , where the first term is the cost of acceleration, and the second term $\mathcal{C}(x_t, v_t; f_t)$ describes the agent's position and velocity's misalignment from a given distribution f_t :

$$\begin{aligned} \mathcal{C}(x, v; f) &= \left\| \int_{\mathbb{R}^{2n}} w(\|x - x'\|)(v' - v) f(x', v') dx' dv' \right\|_Q^2 \\ &= \left\| \tilde{\mathbb{E}}_{(x', v') \sim f} [w(\|x - x'\|)(v' - v)] \right\|_Q^2. \end{aligned}$$

Here $w(x) := \frac{1}{(1+x^2)^\beta}$ ($\beta \geq 0$), the expectation $\tilde{\mathbb{E}}$ is with respect to the distribution f , and Q, R are symmetric positive definite matrices with compatible dimensions such that $\|x\|_Q := (x^\top Q x)^{1/2}$. In order to find the equilibrium of the mean-field game, one needs to find the optimal \hat{u}_t such that f_t is the density of the associated optimal position and velocity (\hat{x}_t, \hat{v}_t) . We remark that our setting is a stochastic MFG on the finite horizon $[0, T]$, while in [39, 40], the authors formulate it as an ergodic mean-field control problem. The infinite horizon MFG was studied in [42] via reinforcement deep learning, deterministic MFGs of Cucker-Smale model on finite horizon was also studied in the past [46, 4].

4.2.1 The Reformulation through MV-FBSDEs

We can use the stochastic maximum principle [11, Section 3.3.2] to characterize the mean-field equilibrium through MV-FBSDEs. To this end, let us define the Hamiltonian H by

$$H(t, x, v, f, y, u) = (v^\top, u^\top) y + \mathcal{C}(x, v; f) + \|u\|_R^2,$$

where $y \in \mathbb{R}^{2n}$. Denote by $y_{1:n}$ the first half entries of this vector and by $y_{n+1:2n}$ the second half, then the unique minimizer of H is given by:

$$\hat{u} = -\frac{1}{2} R^{-1} y_{n+1:2n}.$$

With straightforward computation, the derivatives of H with respect to the state variables (x, v) are:

$$\begin{aligned} \partial_x H &= \partial_x \mathcal{C}(x, v; f) \\ &= 2 \tilde{\mathbb{E}}_{(x', v') \sim f} [\partial_x w(\|x - x'\|)(v' - v)]^\top Q \tilde{\mathbb{E}}_{(x', v') \sim f} [w(\|x - x'\|)(v' - v)], \\ \partial_v H &= y_{1:n} + \partial_v \mathcal{C}(x, v; f) \\ &= y_{1:n} + 2Q \tilde{\mathbb{E}}_{(x', v') \sim f} [w(\|x - x'\|)(v' - v)] \tilde{\mathbb{E}}_{(x', v') \sim f} [-w(\|x - x'\|)], \end{aligned}$$

where $\partial_x w(\|x - x'\|)(v' - v)$ is understood as a Jacobian matrix

$$\begin{bmatrix} \frac{\partial w(\|x-x'\|)}{\partial x_1}(v'_1 - v_1) & \cdots & \frac{\partial w(\|x-x'\|)}{\partial x_n}(v'_1 - v_1) \\ \vdots & \cdots & \vdots \\ \frac{\partial w(\|x-x'\|)}{\partial x_1}(v'_n - v_n) & \cdots & \frac{\partial w(\|x-x'\|)}{\partial x_n}(v'_n - v_n) \end{bmatrix},$$

and x_i, v_i denotes the i^{th} entry of x, v , respectively.

By the stochastic maximum principle, $(\hat{u}_t, \hat{f}_t)_{0 \leq t \leq T}$ is an MFG equilibrium if and only if $\hat{u}_t = -\frac{1}{2}R^{-1}Y_t^2$, $\hat{f}_t = \mathcal{L}(x_t, v_t)$ and (x_t, v_t, Y_t, Z_t) solves the MV-FBSDEs

$$\begin{cases} dx_t = v_t dt, & dv_t = -\frac{1}{2}R^{-1}Y_t^2 dt + C dW_t, & (x_0, v_0) = \xi, \\ dY_t = -\begin{pmatrix} \partial_x H \\ \partial_v H \end{pmatrix}(t, x_t, v_t, \mathcal{L}(x_t, v_t), Y_t, \hat{u}_t) dt + Z_t dW_t, & Y_T = 0, \end{cases} \quad (31)$$

where $Y_t \in \mathbb{R}^{2n}$ is the backward process with $Y_t^1 \in \mathbb{R}^n, Y_t^2 \in \mathbb{R}^n$ be the first half and second half entries, and $Z_t = \begin{pmatrix} Z_t^1 \\ Z_t^2 \end{pmatrix} \in \mathbb{R}^{2n \times p}$ is the adjoint process with Z_t^1 and Z_t^2 being $\mathbb{R}^{n \times p}$ -valued.

Therefore the distribution dependence functions are identified as

$$\begin{aligned} m_1 &\equiv 0, & m_3 &\equiv 0, \\ m_2(t, x_t, v_t, \mathcal{L}(x_t, v_t)) &= \begin{bmatrix} \tilde{\mathbb{E}}[\partial_x w(\|x_t - x'_t\|)(v'_t - v_t)]^T Q \tilde{\mathbb{E}}[w(\|x_t - x'_t\|)(v'_t - v_t)] \\ \tilde{\mathbb{E}}[w(\|x_t - x'_t\|)(v'_t - v_t)] \tilde{\mathbb{E}}[-w(\|x_t - x'_t\|)] \end{bmatrix}, \end{aligned}$$

where (x'_t, v'_t) is a copy of (x_t, v_t) and $\tilde{\mathbb{E}}$ is with respect to (x'_t, v'_t) distributed according to $\mathcal{L}(x_t, v_t)$.

The system (31) hardly admits an explicit solution in general. A special case is when $\beta = 0$, $w(x) \equiv 1$, and the problem reduces to a linear-quadratic mean-field game in which the mean-field cost-coupling function becomes

$$\mathcal{C}(x, v; f) = \left\| \tilde{\mathbb{E}}_{(x', v') \sim f}[v' - v] \right\|_Q^2 = \|\mathbb{E}[v] - v\|_Q^2.$$

The derivatives of Hamiltonian are then simplified to

$$\partial_x H = 0, \quad \partial_v H = y_{1:n} + 2Q(v - \tilde{\mathbb{E}}_{(x', v') \sim f}[v']) = y_{1:n} + 2Q(v - \mathbb{E}[v]).$$

Now the FBSDEs derived from the stochastic maximum principle become

$$\begin{cases} dx_t = v_t dt, & dv_t = -\frac{1}{2}R^{-1}Y_t^2 dt + C dW_t, & (x_0, v_0) = \xi, \\ dY_t = -\begin{pmatrix} 0 \\ Y_t^1 + 2Q(v_t - \mathbb{E}[v_t]) \end{pmatrix} dt + Z_t dW_t, & Y_T = 0, \end{cases} \quad (32)$$

where one immediately deduces $Y_t^1 \equiv Z_t^1 \equiv 0$. We then only need to solve the forward-backward system of (v_t, Y_t^2) only. Let the ansatz of Y_t^2 be

$$Y_t^2 = \eta(t)v_t + \chi(t), \quad \eta(T) = \chi(T) = 0,$$

where $\eta(t) \in \mathbb{R}^{n \times n}$ and $\chi(t) \in \mathbb{R}^n$. Plugging it back to (32) gives the following system:

$$\begin{cases} \dot{\eta}(t) - \frac{1}{2}\eta(t)R^{-1}\eta(t) + 2Q = 0, & \eta(T) = 0, \\ \dot{\chi}(t) - \frac{1}{2}\eta(t)R^{-1}\chi(t) - 2Q\mathbb{E}[v_0] = 0, & \chi(T) = 0. \end{cases}$$

One can also deduce that $Z_t^2 = \eta(t)C$, $\mathbb{E}[Y_t^2] \equiv 0$ and $\mathbb{E}[v_t] \equiv \mathbb{E}[v_0]$. The solution to the above analytical matrix Riccati equation serves as the benchmark solution to the experiment below when $\beta = 0$.

4.2.2 Numerical Results

We use the proposed method to solve the problem numerically with $n = p = 3$, and choose $Q = I_3$, $R = 0.5I_3$, $C = 0.1I_3$, $T = 1$, and $\beta = 0, 0.1, 0.2, 0.3$, where I_3 denotes the identity matrix of size 3. Thus, the solution to (31) is of dimension $\mathbb{R}^6 \times \mathbb{R}^6 \times \mathbb{R}^{6 \times 3}$. We assume $x_0 \sim \mathcal{N}(0, I_3)$, $v_0 \sim \mathcal{N}(1, I_3)$. We discretize the time interval $[0, 1]$ into 50 equal subintervals and simulate $N = 1000$ SDE paths to approximate the state distribution $\mathcal{L}(x_t, v_t)$. We use feedforward neural networks with two hidden layers of width 48 and Rectified Linear Unit (ReLU) activation function to approximate the unknown functions in the BSDE solver and \mathfrak{m}_2 when approximating the distribution dependence. The fictitious play is run for 60 stages and the total runtime is 474 seconds (implemented on a Macbook Pro with a 2.40 Gigahertz Intel Core i9 processor). The numerical solution of $\beta = 0$ is very close to the analytical solution, with an L^2 error of Y_0^2 being 0.017.

In the left and middle panels of Figure 3, we plot the density of the final position x_T and the final velocity v_T . Since we choose the parameter such that the problem is symmetric with three dimensions, we only present the first entry of x_T and v_T . In the right panel of Figure 3, we present the standard deviation of v_t 's first entry as a function of time t with different β . From all three subplots in Figure 3 we can see that, when $\beta = 0$, the analytical solution and our numerical solution agree very well with each other. We also observe that the standard deviation of v increases as β increases. This qualitative trend is consistent with our intuition since the cost of ‘‘misalignment’’ of the location-velocity decreases as β increases. This intuition is further confirmed in Figure 4, in which we plot the density of the control u_t 's first entry at $t = 0.0, 0.3, 0.6$. It is mathematically clear that as β increases, the second cost term $\mathcal{C}(x_t, v_t; f_t)$ in equation (30) punishes the location-velocity ‘‘misalignment’’ less severe. Thus the agents will not spend as much effort (large acceleration u_t) as they would for smaller β , as they also want to minimize first cost term $\|u\|_R^2$ in (30). As a result, the density of u_t is more centered at 0 for large β .

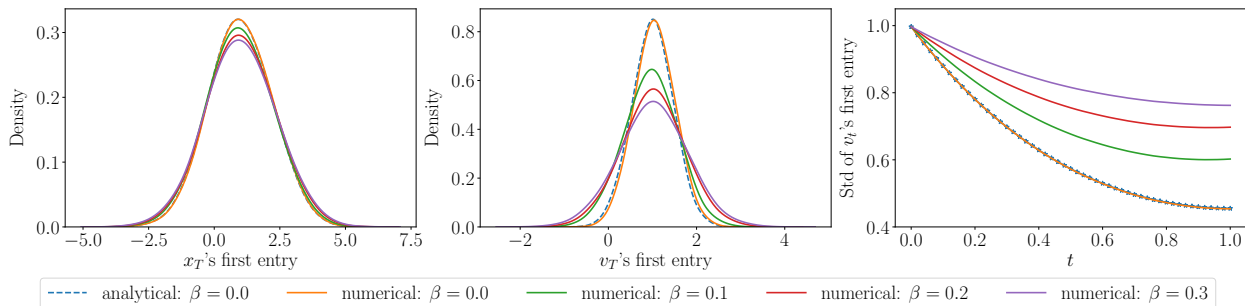


Figure 3: Numerical solution of the states to the Cucker-Smale MFG (31). Left: the density of the position x_T 's first entry with different β . Middle: the density of the velocity v_T 's first entry with different β . Right: the standard deviation of v_t 's first entry as a function of time with different β .

5 Conclusion

Built on deep learning BSDE solvers, we propose a novel deep learning method for solving the McKean-Vlasov forward-backward stochastic differential equations, which have been frequently

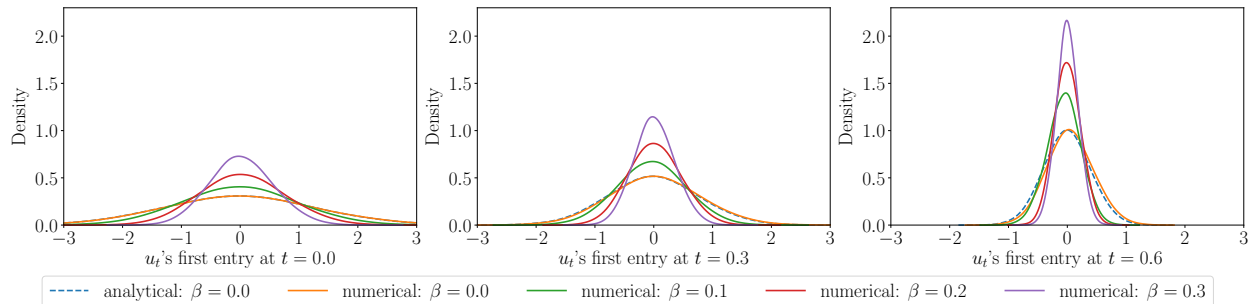


Figure 4: Numerical solution of the optimal control to the Cucker-Smale MFG (31). From left to right: the density of u_t 's first entry with different β at different time $t = 0.0, 0.3, 0.6$.

used in mean-field control problems and mean-field games. Specifically, we can compute the general cases when the mean-field interactions depend on full distributions, not only on expectation or other moments. We prove that the convergence of the proposed method is free of the curse of dimensionality by using a class of integral probability metrics [25]. The proved theorem shows the advantage of the method in high dimensions. We then derived a mean-field game of the well-known Cucker-Smale model, with the cost depending on the full distribution of the forward process. The numerical results are nicely in line with the model's intuition. In the future, we plan to study numerical algorithms for MV-FBSDEs where the dependence of $\mathcal{L}(X_t)$ is not by the integral form, but via $f(X_t)$ where $f(\cdot)$ is the density or cumulative distribution function of the forward process X_t . This is motivated by the famous beach towel mean-field game [36]. Another plan is to extend the algorithm to MV-FBSDEs in a random environment, corresponding to mean-field control and game problems with a common noise.

Acknowledgments

R.H. was partially supported by the NSF grant DMS-1953035, the Faculty Career Development Award, the Research Assistance Program Award, the Early Career Faculty Acceleration funding and the Regents' Junior Faculty Fellowship at the University of California, Santa Barbara, and a grant from the Simons Foundation (MP-TSM-00002783).

References

- [1] Yves Achdou, Jiequn Han, Jean-Michel Lasry, Pierre-Louis Lions, and Benjamin Moll. Income and wealth distribution in macroeconomics: A continuous-time approach. *The Review of Economic Studies*, 89(1):45–86, 2022.
- [2] Yves Achdou and Mathieu Laurière. Mean field games and applications: Numerical aspects. *Mean field games*, pages 249–307, 2020.
- [3] M. Arjovsky, S. Chintala, and L. Bottou. Wasserstein generative adversarial networks. In *Proceedings of the 34th International Conference on Machine Learning*, volume 70 of *PLMR*, pages 214–223, 2017.
- [4] Martino Bardi and Pierre Cardaliaguet. Convergence of some mean field games systems to aggregation and flocking models. *Nonlinear Analysis*, 204:112199, 2021.

- [5] Christian Bender and Jianfeng Zhang. Time discretization and markovian iteration for coupled FBSDEs. *The Annals of Applied Probability*, 18(1):143–177, 2008.
- [6] George W Brown. Some notes on computation of games solutions. Technical report, RAND CORP SANTA MONICA CA, 1949.
- [7] George W Brown. Iterative solution of games by fictitious play. *Activity Analysis of Production and Allocation*, 13(1):374–376, 1951.
- [8] René Carmona and François Delarue. Mean field forward-backward stochastic differential equations. *Electronic Communications in Probability*, 18:1–15, 2013.
- [9] René Carmona and François Delarue. Probabilistic analysis of mean-field games. *SIAM Journal on Control and Optimization*, 51(4):2705–2734, 2013.
- [10] René Carmona and François Delarue. Forward–backward stochastic differential equations and controlled McKean–Vlasov dynamics. *The Annals of Probability*, 43(5):2647–2700, 2015.
- [11] René Carmona and François Delarue. *Probabilistic Theory of Mean Field Games with Applications I*. Springer, 2017.
- [12] René Carmona and Mathieu Laurière. Convergence analysis of machine learning algorithms for the numerical solution of mean field control and games: II—the finite horizon case. *arXiv preprint arXiv:1908.01613*, 2019.
- [13] Jean-François Chassagneux, Dan Crisan, and François Delarue. Numerical method for FBSDEs of McKean–Vlasov type. *The Annals of Applied Probability*, 29(3):1640–1684, 2019.
- [14] Felipe Cucker and Steve Smale. On the mathematics of emergence. *Japanese Journal of Mathematics*, 2(1):197–227, 2007.
- [15] PE Chaudru de Raynal and CA Garcia Trillos. A cubature based algorithm to solve decoupled McKean–Vlasov forward–backward stochastic differential equations. *Stochastic Processes and their Applications*, 125(6):2206–2255, 2015.
- [16] Weinan E, Jiequn Han, and Arnulf Jentzen. Deep learning-based numerical methods for high-dimensional parabolic partial differential equations and backward stochastic differential equations. *Communications in Mathematics and Statistics*, 5(4):349–380, 2017.
- [17] Weinan E, Chao Ma, and Lei Wu. The Barron space and the flow-induced function spaces for neural network models. *arXiv preprint arXiv:1906.08039*, 2019.
- [18] Romuald Elie, Julien Pérolat, Mathieu Laurière, Matthieu Geist, and Olivier Pietquin. Approximate fictitious play for mean field games. In *Accepted for an oral presentation at the Thirty-Fourth AAAI Conference on Artificial Intelligence (AAAI-20)*, June 2020.
- [19] M. Fazlyab, A. Robey, H. Hassani, M. Morari, and G. Pappas. Efficient and accurate estimation of Lipschitz constants for deep neural networks. In *Advances in Neural Information Processing Systems*, pages 11427–11438, 2019.
- [20] Chris Finlay, Jeff Calder, Bilal Abbasi, and Adam Oberman. Lipschitz regularized deep neural networks generalize and are adversarially robust. *arXiv preprint arXiv:1808.09540*, 2018.

- [21] Maximilien Germain, Joseph Mikael, and Xavier Warin. Numerical resolution of McKean-Vlasov FBSDEs using neural networks. *arXiv preprint arXiv:1909.12678*, 2019.
- [22] I. Gulrajani, F. Ahmed, M. Arjovsky, V. Dumoulin, and A. C. Courville. Improved training of Wasserstein GANs. In *Advances in neural information processing systems*, pages 5767–5777, 2017.
- [23] Jiequn Han and Ruimeng Hu. Deep fictitious play for finding Markovian Nash equilibrium in multi-agent games. In *Proceedings of The First Mathematical and Scientific Machine Learning Conference (MSML)*, volume 107, pages 221–245, 2020.
- [24] Jiequn Han, Ruimeng Hu, and Jihao Long. Convergence of deep fictitious play for stochastic differential games. *arXiv preprint arXiv:2008.05519*, 2020.
- [25] Jiequn Han, Ruimeng Hu, and Jihao Long. A class of dimensionality-free metrics for the convergence of empirical measures. *arXiv preprint arXiv:2104.12036*, 2021.
- [26] Jiequn Han, Arnulf Jentzen, and Weinan E. Solving high-dimensional partial differential equations using deep learning. *Proceedings of the National Academy of Sciences*, 115(34):8505–8510, 2018.
- [27] Jiequn Han and Jihao Long. Convergence of the deep BSDE method for coupled FBSDEs. *Probability, Uncertainty and Quantitative Risk*, 5(1):1–33, 2020.
- [28] Jiequn Han, Yucheng Yang, and Weinan E. Deepham: A global solution method for heterogeneous agent models with aggregate shocks. *arXiv preprint arXiv:2112.14377*, 2021.
- [29] Ruimeng Hu. Deep fictitious play for stochastic differential games. *Communications in Mathematical Sciences*, 19(2):325–353, 2021.
- [30] Minyi Huang, Peter E Caines, and Roland P Malhamé. Large population stochastic dynamic games: closed-loop McKean-Vlasov systems and the Nash certainty equivalence principle. *Communications in Information and Systems*, 6(3):221–252, 2006.
- [31] Minyi Huang, Peter E Caines, and Roland P Malhamé. Large-population cost-coupled LQG problems with nonuniform agents: Individual-mass behavior and decentralized ϵ -Nash equilibria. *IEEE Transactions on Automatic Control*, 52(9):1560–1571, 2007.
- [32] Côme Huré, Huyên Pham, and Xavier Warin. Deep backward schemes for high-dimensional nonlinear pdes. *Mathematics of Computation*, 89(324):1547–1579, 2020.
- [33] Jean-Michel Lasry and Pierre-Louis Lions. Jeux à champ moyen. I. Le cas stationnaire. *C. R. Math. Acad. Sci. Paris*, 9:619–625, 2006.
- [34] Jean-Michel Lasry and Pierre-Louis Lions. Jeux à champ moyen. II. Horizon fini et contrôle optimal. *C. R. Math. Acad. Sci. Paris*, 10:679–684, 2006.
- [35] Jean-Michel Lasry and Pierre-Louis Lions. Mean field games. *Japanese Journal of Mathematics*, 2:229–260, 2007.
- [36] PL Lions. Théorie des jeux champs moyen et applications. *Cours au Collège de France*, www.college-de-france.fr, 2007.

- [37] Ming Min and Ruimeng Hu. Signed deep fictitious play for mean field games with common noise. In *Proceedings of the 38th International Conference on Machine Learning*, pages 7736–7747. PMLR, 2021.
- [38] Alfred Müller. Integral probability metrics and their generating classes of functions. *Advances in Applied Probability*, 29(2):429–443, 1997.
- [39] Mojtaba Nourian, Peter E Caines, and Roland P Malhamé. Synthesis of cucker-smale type flocking via mean field stochastic control theory: Nash equilibria. In *2010 48th Annual Allerton Conference on Communication, Control, and Computing (Allerton)*, pages 814–819. IEEE, 2010.
- [40] Mojtaba Nourian, Peter E Caines, and Roland P Malhamé. Mean field analysis of controlled cucker-smale type flocking: Linear analysis and perturbation equations. *IFAC Proceedings Volumes*, 44(1):4471–4476, 2011.
- [41] Patricia Pauli, Anne Koch, Julian Berberich, Paul Kohler, and Frank Allgöwer. Training robust neural networks using Lipschitz bounds. *IEEE Control Systems Letters*, 6:121–126, 2021.
- [42] Sarah Perrin, Mathieu Laurière, Julien Pérolat, Matthieu Geist, Romuald Élie, and Olivier Pietquin. Mean field games flock! the reinforcement learning way. *Accepted at the 30th International Joint Conference on Artificial Intelligence (IJCAI-21)*. *arXiv preprint arXiv:2105.07933*, 2021.
- [43] Christoph Reisinger, Wolfgang Stockinger, and Yufei Zhang. Path regularity of coupled McKean-Vlasov FBSDEs. *arXiv preprint arXiv:2011.06664*, 2020.
- [44] Christoph Reisinger, Wolfgang Stockinger, and Yufei Zhang. A fast iterative PDE-based algorithm for feedback controls of nonsmooth mean-field control problems. *arXiv preprint arXiv:2108.06740*, 2021.
- [45] Lars Ruthotto, Stanley J Osher, Wuchen Li, Levon Nurbekyan, and Samy Wu Fung. A machine learning framework for solving high-dimensional mean field game and mean field control problems. *Proceedings of the National Academy of Sciences*, 117(17):9183–9193, 2020.
- [46] Filippo Santambrogio and Woojoo Shim. A Cucker–Smale inspired deterministic mean field game with velocity interactions. *SIAM Journal on Control and Optimization*, 59(6):4155–4187, 2021.
- [47] Qiaomin Xie, Zhuoran Yang, Zhaoran Wang, and Andreea Minca. Provable fictitious play for general mean-field games. *arXiv preprint arXiv:2010.04211*, 2020.
- [48] Yao Xuan, Robert Balkin, Jiequn Han, Ruimeng Hu, and Hector D. Ceniceros. Optimal policies for a pandemic: A stochastic game approach and a deep learning algorithm. In *Proceedings of The Second Mathematical and Scientific Machine Learning Conference (MSML)*, 2021. Accepted.
- [49] Jianfeng Zhang. *Backward Stochastic Differential Equations*. Springer New York, 2017.